

Supporting Information for

Fusing Triphenylphosphine with Tetrphenylborate: Introducing the 9-Phosphatriptycene-10-Phenylborate (PTB) Anion

Marcus W. Drover,[†] Koichi Nagata,[†] and Jonas C. Peters^{*}

[†]These authors contributed equally

*E-mail: jpeters@caltech.edu

*Division of Chemistry and Chemical Engineering, California Institute of Technology,
Pasadena, California, 91125, United States

1. General Considerations	S2
2. Synthetic Procedures	S3
3. Electrochemistry	S30
4. Crystallography Discussion and Tables	S31
5. Density Functional Theory	S36
6. References	S37

General Considerations:

All experiments were carried out employing standard Schlenk techniques under an atmosphere of dry nitrogen or argon employing degassed, dried solvents in a solvent purification system supplied by SG Water, LLC. Non-halogenated solvents were tested with a standard purple solution of sodium benzophenone ketyl in THF in order to confirm effective moisture removal. $P(o\text{-BrC}_6\text{H}_4)_3$,¹ 5-azoniaspiro[4.4]nonane bromide ($[\text{ASN}]\text{Br}$)², and $\text{W}(\text{CO})_5\text{THF}$ were prepared according to a literature procedure. All other reagents were purchased from commercial vendors and used without further purification unless otherwise stated.

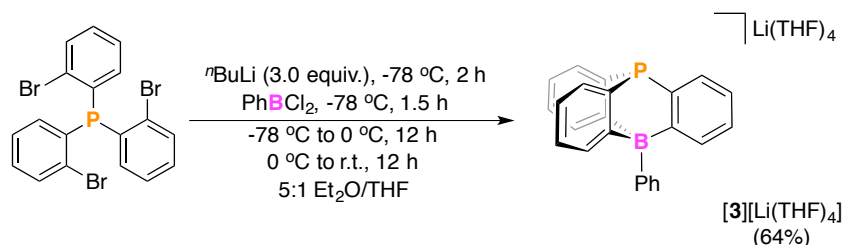
Physical methods:

Fourier transform infrared ATR (FT-IR ATR) spectra were collected on a Bruker Alpha Platinum ATR spectrometer using OPUS software. NMR data were collected on a Varian 300 or 400 MHz instrument with chemical shifts reported in ppm relative to deuterated solvent, using residual solvent resonances as internal standards. ³¹P chemical shifts are reported in ppm relative to 85% aqueous H₃PO₄. UV-Visible spectroscopy measurements were collected with a Cary 50 UV-Vis spectrophotometer using a 1 cm two-window quartz cell.

- ⁵⁷Fe Mössbauer:

Mössbauer spectra were recorded on a spectrometer from SEE Co. (Edina, MN) operating in the constant acceleration mode in transmission geometry. The sample was kept in an SVT-400 cryostat from Janis (Wilmington, MA), using liquid N₂ as a cryogen for 80 K measurements. The quoted isomer shifts are relative to the centroid of the spectrum of a metallic foil of α -Fe at room temperature. Solution samples were transferred to a sample cup and chilled to 77 K inside of the glovebox, and quickly removed from the glovebox and immersed in liquid N₂ until mounted in the cryostat. Data analysis was performed using WMOSS version 4 (www.wmoss.org) and quadrupole doublets were fit to Lorentzian lineshapes.³

Synthetic Procedures:



Tetrakis(tetrahydrofuran) lithium phosphatriptycene-10-phenylborate ([3][Li(THF)₄]): A solution of *n*BuLi (1.6 M, 1.1 mL, 1.7 mmol) in hexane was added dropwise to a solution of *tris*(2-bromophenyl)phosphine¹ (288 mg, 578.0 μmol) in Et₂O (80 mL) and THF (24 mL) at -78 °C. Following addition, the resulting mixture was stirred for an additional 2 h at -78 °C and a solution of PhBCl₂ (70.0 μL, 578 μmol) in Et₂O (20 mL) was added drop wise to the mixture at -78 °C. Subsequently, the mixture was allowed to warm to 0 °C and then stirred for an additional 24 h. Next, all volatiles were removed *in-vacuo* and the residue was dissolved in C₆H₆ and filtered through a pad of Celite[®]. The resulting pale yellow solid was dissolved in THF and again filtered through a pad of Celite[®]. Concentration of the filtrate and cooling at -35 °C afforded [3][Li(THF)₄] as a pale yellow solid (238 mg, 64%).

¹H NMR (CD₃CN, 400 MHz, 298 K): δ = 8.10 (br, 2H; *o*-Ph), 7.65 (d, ³J_{H,H} = 7.2 Hz, 3H), 7.47 (br, 2H), 7.45 (t, ³J_{H,H} = 7.2 Hz, 3H; *m*-Ph), 7.26 (t, ³J_{H,H} = 7.2 Hz, 1H; *p*-Ph), 6.91 (t, ³J_{H,H} = 7.2 Hz, 3H), 6.83 (t, ³J_{H,H} = 7.2 Hz, 3H), 3.71 (m, 16H, THF), 1.84 (m, 16H, THF).

⁷Li{¹H} NMR (CD₃CN, 156 MHz, 298 K): δ = -1.2.

³¹P{¹H} NMR (THF-*d*₈, 162 MHz, 298 K): δ = -43.7 (d, ³J_{P,B} = 3.8 Hz).

¹¹B{¹H} NMR (CD₃CN, 128 MHz, 298 K): δ = -8.75 (d, ³J_{P,B} = 3.8 Hz).

¹³C NMR (THF-*d*₈, 100 MHz, 298 K): δ = 147.3, 137.4, 132.1, 131.6, 131.5, 126.5, 124.9, 122.7, 120.8, 120.7, 58.6, 46.0.

HR ESI(-)-MS: Calcd. 347.1838 for C₂₄H₁₇BP [3]⁻. Found. 347.1814

Figure S1. [3][Li(THF)₄], ¹H NMR, CD₃CN, 400 MHz, 298 K

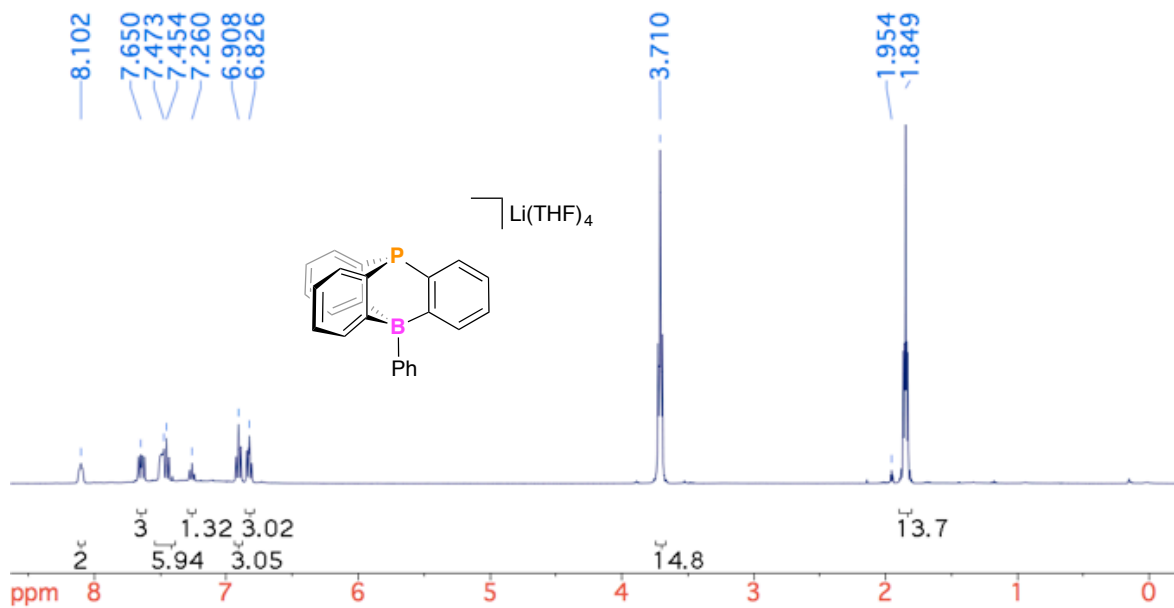


Figure S2. [3][Li(THF)₄], ⁷Li{¹H} NMR, CD₃CN, 156 MHz, 298 K

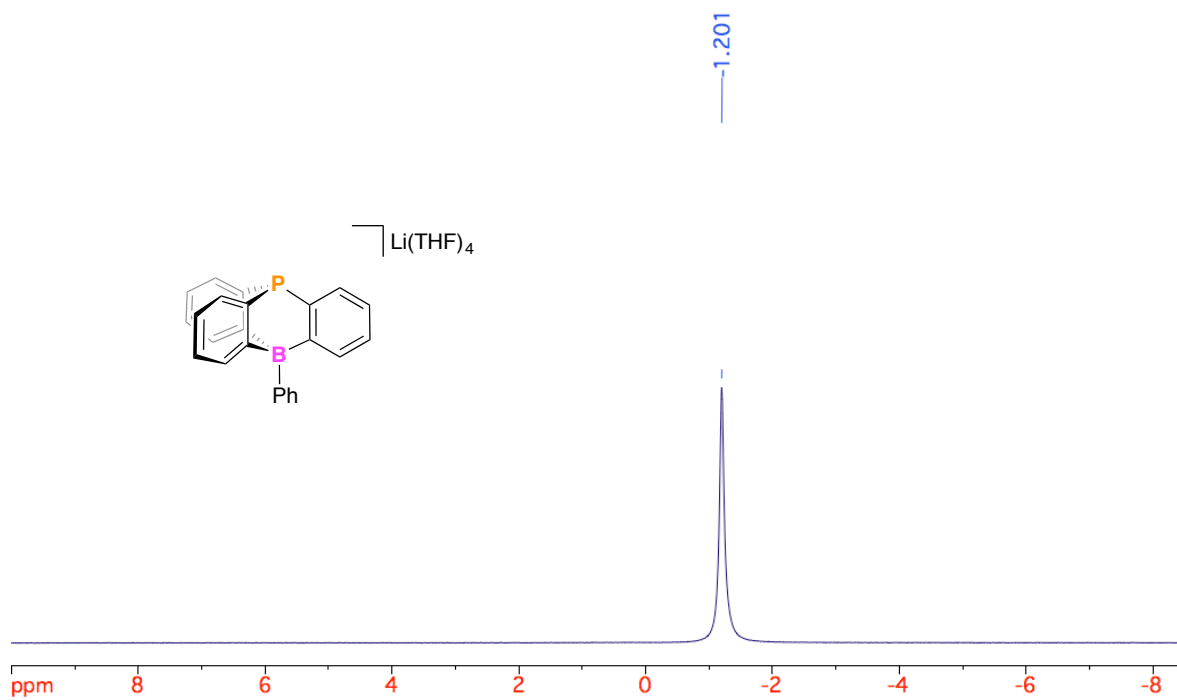


Figure S3. $[3][\text{Li}(\text{THF})_4]$, $^{31}\text{P}\{^1\text{H}\}$ NMR, THF- d_8 , 162 MHz, 298 K

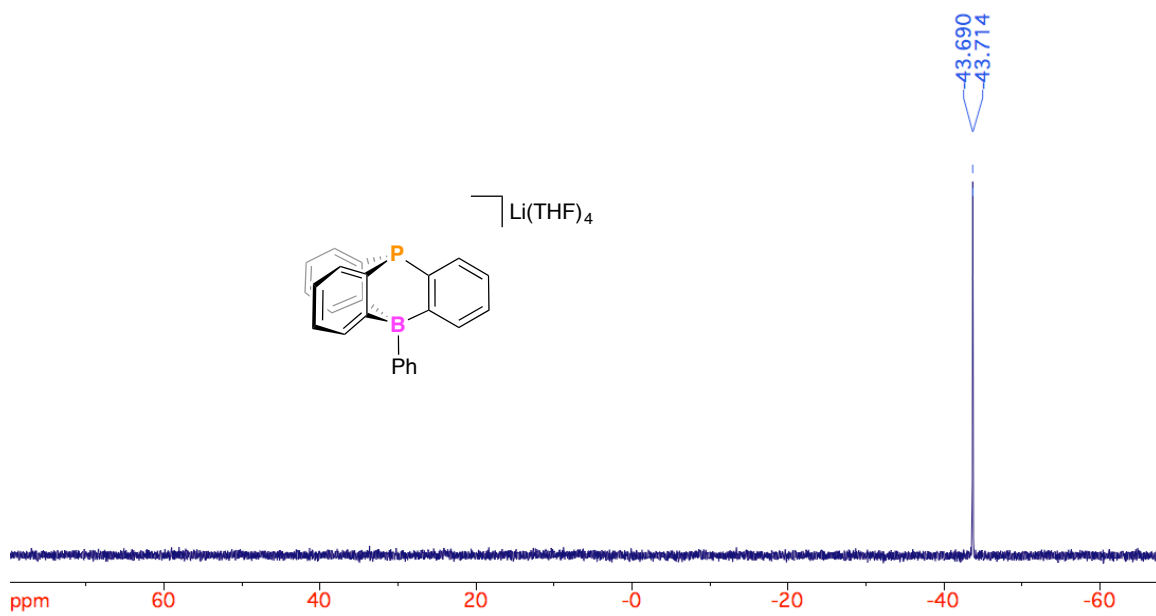


Figure S4. $[3][\text{Li}(\text{THF})_4]$, $^{11}\text{B}\{^1\text{H}\}$ NMR, CD_3CN , 128 MHz, 298 K

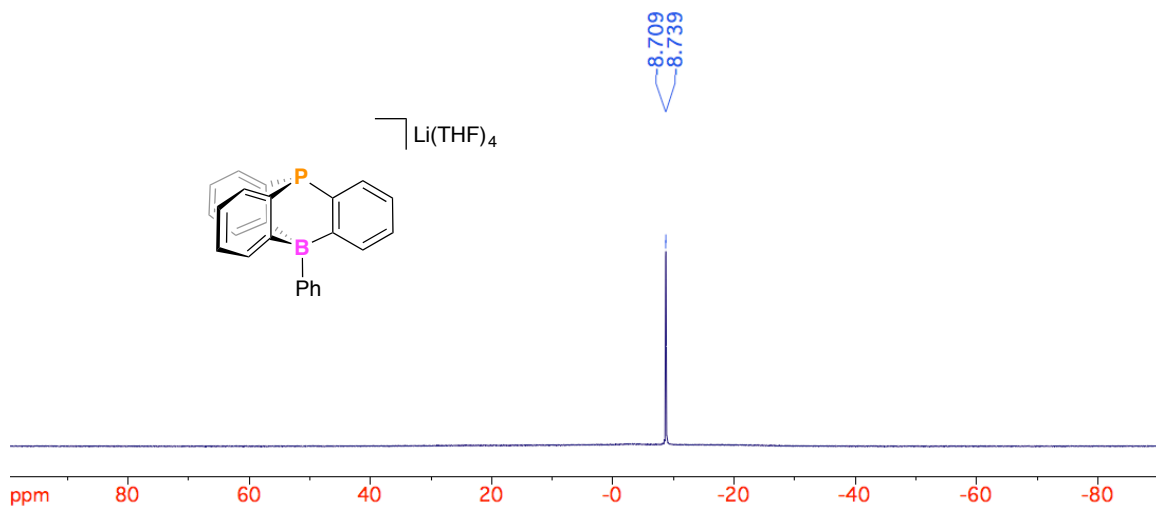
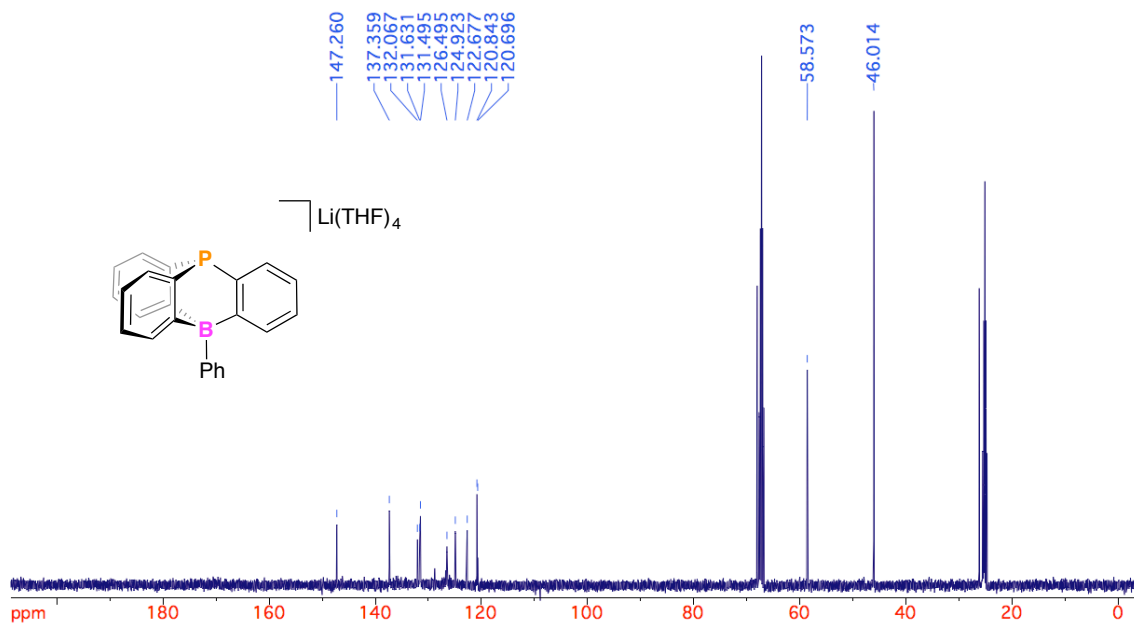
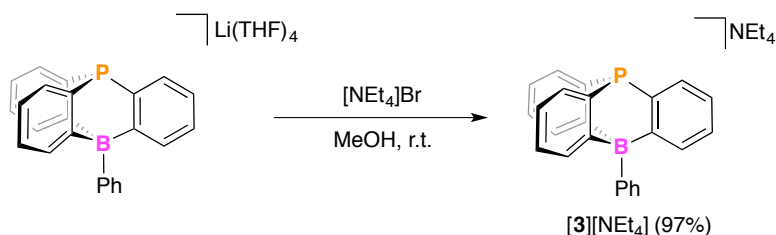
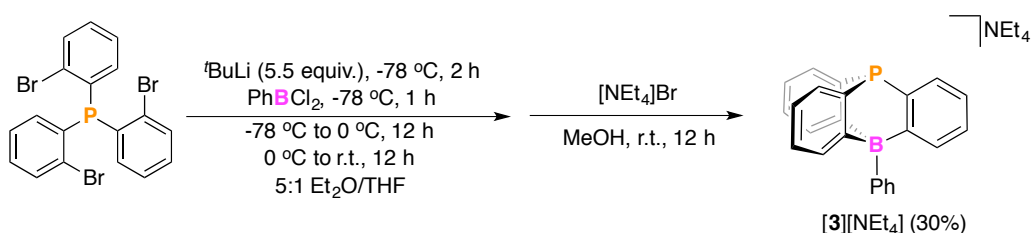


Figure S5. [3][Li(THF)₄], ¹³C{¹H} NMR, THF-d₈, 100 MHz, 298 K





Route A: Tetraethylammonium 9-phosphatriptycene-10-phenylborate ([3][NEt₄]): To a stirring MeOH (1 mL) solution of [3][Li(THF)₄] (13 mg, 20.4 μmol) was added [NEt₄]Br (4.3 mg, 20.4 μmol) in MeOH (1 mL) at room temperature. Within minutes, a white precipitate formed. After 30 min, the resulting white solid was collected by filtration and washed with MeOH (4 × 1 mL). The solids were dried *in-vacuo* providing [3][NEt₄] (12 mg, 97%). The filtrate was concentrated and stored at -35 °C to afford [3][NEt₄] as colorless crystals.



Route B: Tetraethylammonium 9-phosphatriptycene-10-phenylborate ([3][NEt₄]): An oven-dried 1000 mL three-neck flask was fitted with a flow control two-way-glass adapter, rubber septum, and a 100 mL liquid addition funnel capped with a rubber septum. Under an N₂ atmosphere, the flask was charged with *tris*(2-bromophenyl)phosphine¹ (2.044 g, 4.096 mmol), a mixture of Et₂O (600 mL):THF (200 mL), and a magnetic stir bar. The addition funnel was charged with 1.7 M ^tBuLi in pentane (1.7 M, 13.3 mL, 22.5 mmol) and the three-neck flask was cooled in a acetone/dry ice slush bath (~ -78 °C) with vigorous stirring for ~ 10 min. **Addition of ^tBuLi was commenced drop wise over 25 min.** The addition funnel was washed with Et₂O (10 mL) and subsequently added over 3 min, causing a color change to dark green. The reaction mixture was allowed to stir at -78 °C for 2 h. The addition funnel was subsequently charged with distilled PhBCl₂ (0.5 mL, 4.1 mmol) diluted in Et₂O (52 mL). **This solution was added drop wise over 1.25 h to the vigorously stirred reaction mixture, causing a color change to orange.** After the mixture was stirred for an additional 6 h, the mixture was allowed to warm gradually to 0 °C overnight (~ 12 h). The next morning, the mixture was allowed to warm gradually to room temperature. **After 12**

h, the solution was light yellow with ample white precipitate. Solvent was removed *in-vacuo* and the crude mixture of [3][Li(THF)₄] was dissolved in MeOH (30 mL) and stirred for 2 min after which [NEt₄]Br (857.0 mg, 4.096 mmol) was added at room temperature. After the addition was complete, the mixture was stirred for an additional 12 h. Solvent was removed *in-vacuo* and the residue was washed with MeOH and filtered to give ammonium salt [3][NEt₄] (734 mg, 30%) as a white solid.

¹H NMR (CD₃CN, 400 MHz, 298 K): δ = 8.03 (br, 2H; *o*-Ph), 7.58 (d, ³*J*_{H,H} = 7.2 Hz, 3H), 7.38-7.42 (m, 5H), 7.21 (t, ³*J*_{H,H} = 7.2 Hz, 1H; *p*-Ph), 6.86 (t, ³*J*_{H,H} = 7.2 Hz, 3H), 6.77 (t, ³*J*_{H,H} = 7.2 Hz, 3H), 3.06 (q, ³*J*_{H,H} = 7.2 Hz, CH₂(NEt₄), 8H), 1.14 (t, ³*J*_{H,H} = 7.2 Hz, CH₃(NEt₄), 12H).

³¹P{¹H} NMR (CD₃CN, 162 MHz, 298 K): δ = -46.8 (d, ³*J*_{P,B} = 4.0 Hz).

¹¹B{¹H} NMR (CD₃CN, 128 MHz, 298 K): δ = -8.2. (d, ³*J*_{P,B} = 4.0 Hz).

¹³C NMR (CD₃CN, 100 MHz, 298 K): δ = 146.7, 137.2, 132.8, 132.3, 131.7, 127.5, 126.1, 123.9, 122.2, 122.1, 53.0, 7.6.

HR ESI(-)-MS: Calcd. 347.1838 for C₂₄H₁₇BP [3]⁻. Found. 347.2051

Figure S6. [3][NEt₄], ¹H NMR, CD₃CN, 400 MHz, 298 K

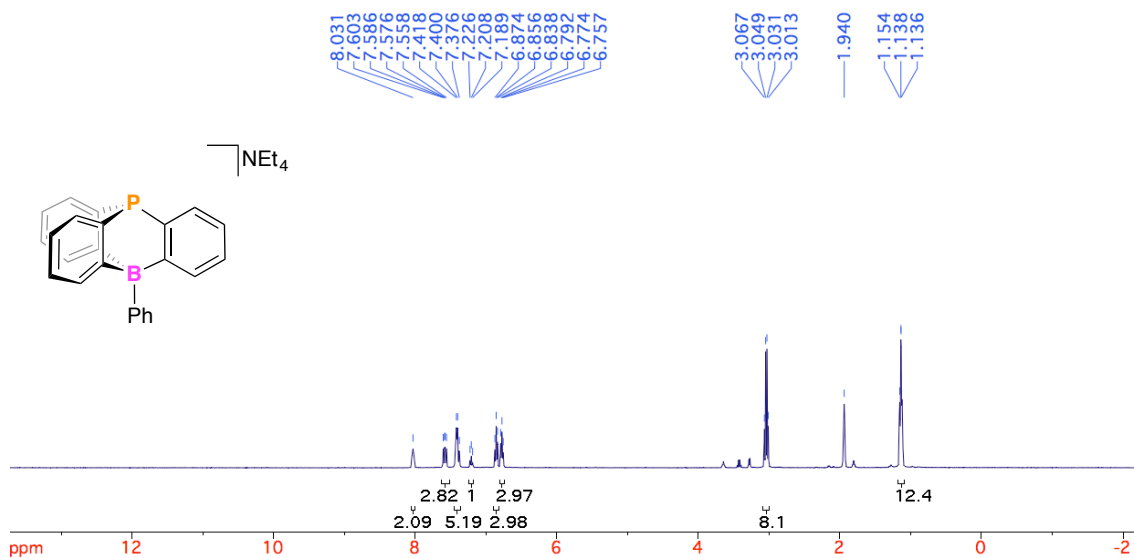


Figure S7. [3][NEt₄], ³¹P{¹H} NMR, CD₃CN, 162 MHz, 298 K

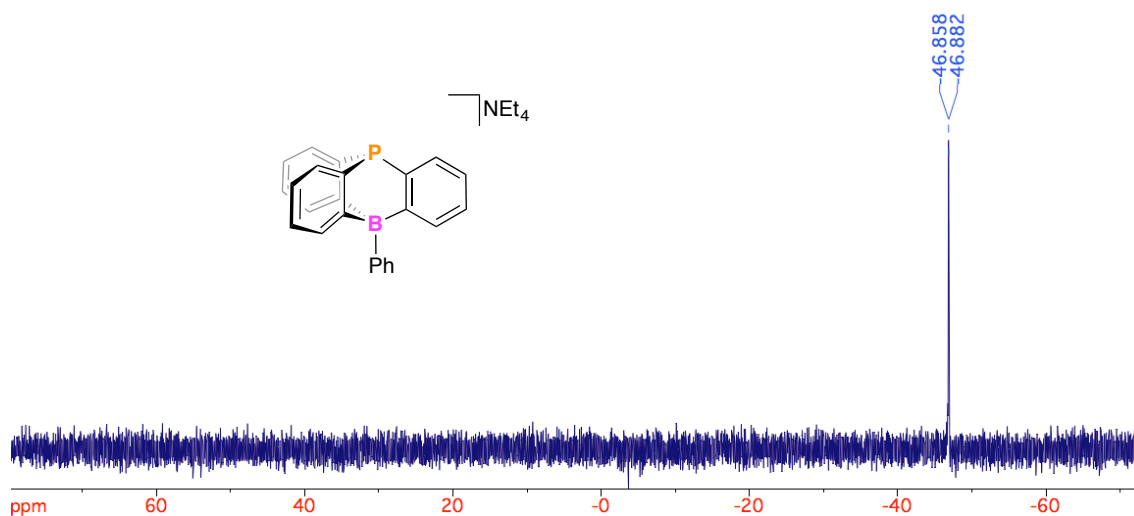


Figure S8. [3][NEt₄], ¹¹B{¹H} NMR, CD₃CN, 128 MHz, 298 K

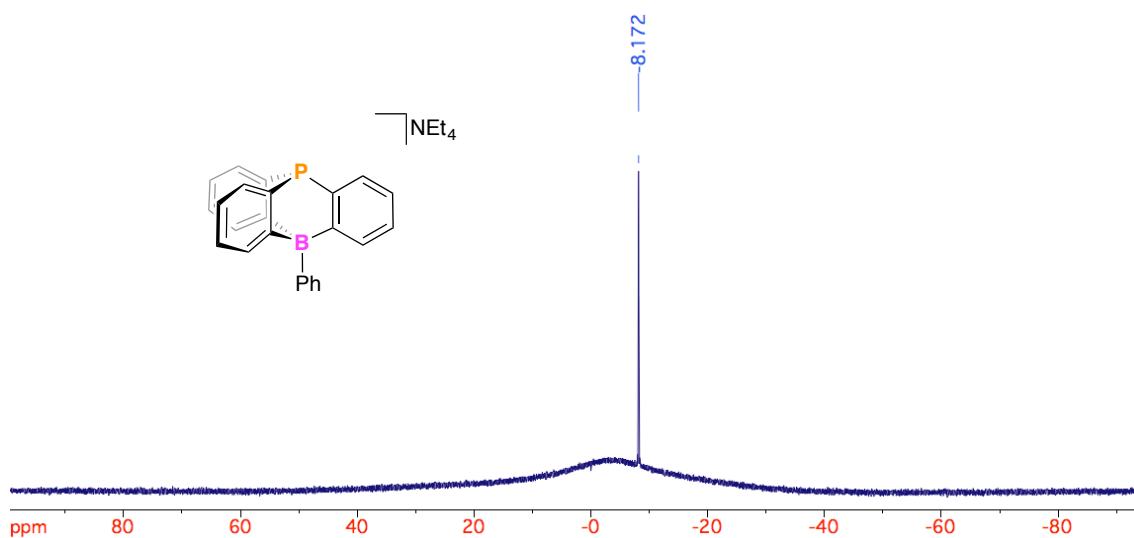
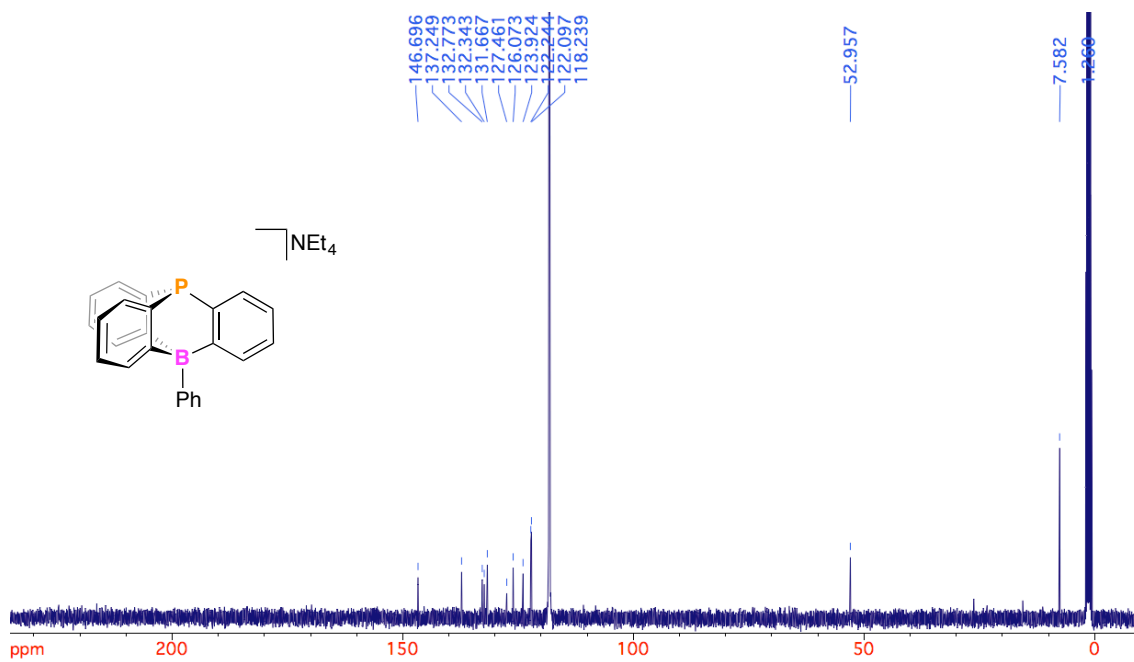
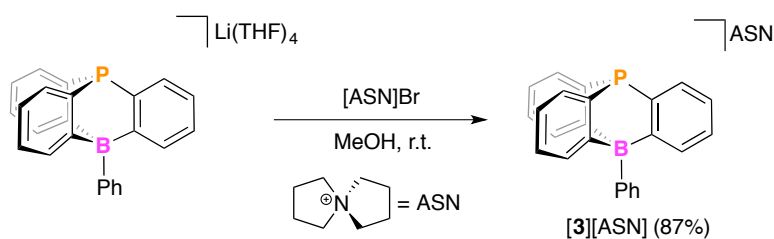
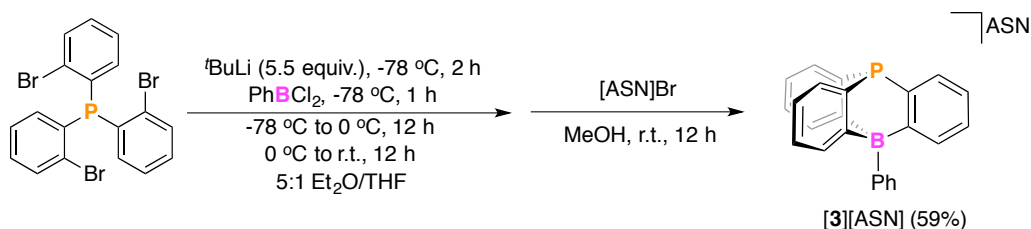


Figure S9. [3][NEt₄], ¹³C{¹H} NMR, CD₃CN, 100 MHz, 298 K





Route A: 5-azoniaspiro[4.4]nonane 9-phosphatriptycene-10-phenylborate (**[3][ASN]**): To a stirring MeOH (2 mL) solution of **[3][Li(THF)₄]** (137 mg, 213.1 μmol) was added **[ASN]Br** (44 mg, 213 μmol) in MeOH (5 mL) at room temperature. Within minutes, a white precipitate formed. After 5 h, the resulting white solid was collected by filtration and washed with MeOH (4×1 mL). The solids were dried *in-vacuo* providing **[3][ASN]** (88 mg, 87%). The filtrate was concentrated and stored at -35 $^\circ\text{C}$ to afford **[3][ASN]** as colorless crystals.



Route B: 5-azoniaspiro[4.4]nonane 9-phosphatriptycene-10-phenylborate (**[3][ASN]**): An oven-dried 2000 mL two-neck flask was fitted with a flow control two-way-glass adapter and a 100 mL liquid addition funnel capped with a rubber septum. Under an N_2 atmosphere, the flask was charged with *tris*(2-bromophenyl)phosphine¹ (4.201 g, 8.420 mmol), a mixture of Et_2O (1200 mL):THF (400 mL), and a magnetic stir bar. The addition funnel was charged with 1.7 M $t\text{BuLi}$ in pentane (1.7 M, 27 mL, 46 mmol) and the two-neck flask was cooled in an acetone/dry ice slush bath (~ -78 $^\circ\text{C}$) with vigorous stirring for ~ 15 min. **Addition of $t\text{BuLi}$ was commenced drop wise over 30 min.** The addition funnel was washed with Et_2O (20 mL) and subsequently added over 3 minutes, causing a color change to dark green (almost black). The reaction mixture was allowed to stir at -78 $^\circ\text{C}$ for 2 h. The addition funnel was subsequently charged with distilled PhBCl_2 (1.3 mL, 8.4 mmol) diluted in Et_2O (100 mL). **This solution was added drop wise over 2 h to the vigorously stirred reaction mixture, causing a color change to orange-red.** After the mixture was stirred for an additional 1 h, the mixture was allowed to warm gradually to 0 $^\circ\text{C}$ overnight (~ 12 h). The next morning, the mixture was allowed to warm gradually to room temperature. **After 12 h, the solution was light orange with ample white precipitate.** Solvent was removed *in-vacuo* and the crude mixture of **[3][Li(THF)₄]** was dissolved in MeOH (40 mL) and stirred for 10 min after which **[ASN]Br** (1.735 g, 8.420 mmol) was added as a solid at room temperature. After the

addition was complete, the mixture was stirred for an additional 12 h. Solvent was removed *in-vacuo* and the residue was washed with MeOH and filtered to give ammonium salt [3][ASN] (2.35 g, 59%) as a white solid.

¹H NMR (CD₃CN, 300 MHz, 298 K): δ = 8.02 (br t, 2H; *o*-Ph), 7.57 (d, ³*J*_{H,H} = 7.2 Hz, 3H), 7.37-7.43 (m, 5H), 7.20 (t, ³*J*_{H,H} = 7.2 Hz, 1H; *p*-Ph), 6.85 (t, ³*J*_{H,H} = 7.2 Hz, 3H), 6.77 (t, ³*J*_{H,H} = 7.2 Hz, 3H), 3.32 (m, 2-H(ASN), 8H), 2.08 (m, 3-H(ASN), 8H).

³¹P{¹H} NMR (CD₃CN, 162 MHz, 298 K): δ = -46.8 (d, ³*J*_{P,B} = 4.0 Hz).

¹¹B{¹H} NMR (CD₃CN, 128 MHz, 298 K): δ = -8.3 (d, ³*J*_{P,B} = 4.0 Hz).

¹³C NMR (CD₃CN, 100 MHz, 298 K): δ = 146.7, 137.3, 132.8, 132.3, 131.7, 129.3, 127.4, 126.1, 123.9, 122.2, 63.7, 22.6.

HR ESI(-)-MS: Calcd. 347.1838 for C₂₄H₁₇BP [3]⁻. Found. 347.1819

Figure S12. [3][ASN], $^{11}\text{B}\{^1\text{H}\}$ NMR, CD_3CN , 128 MHz, 298 K

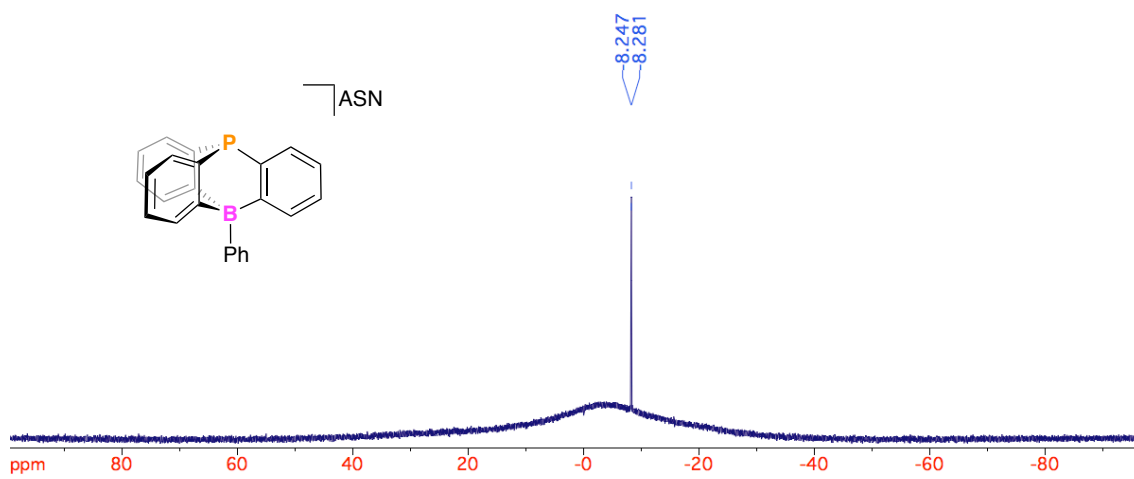
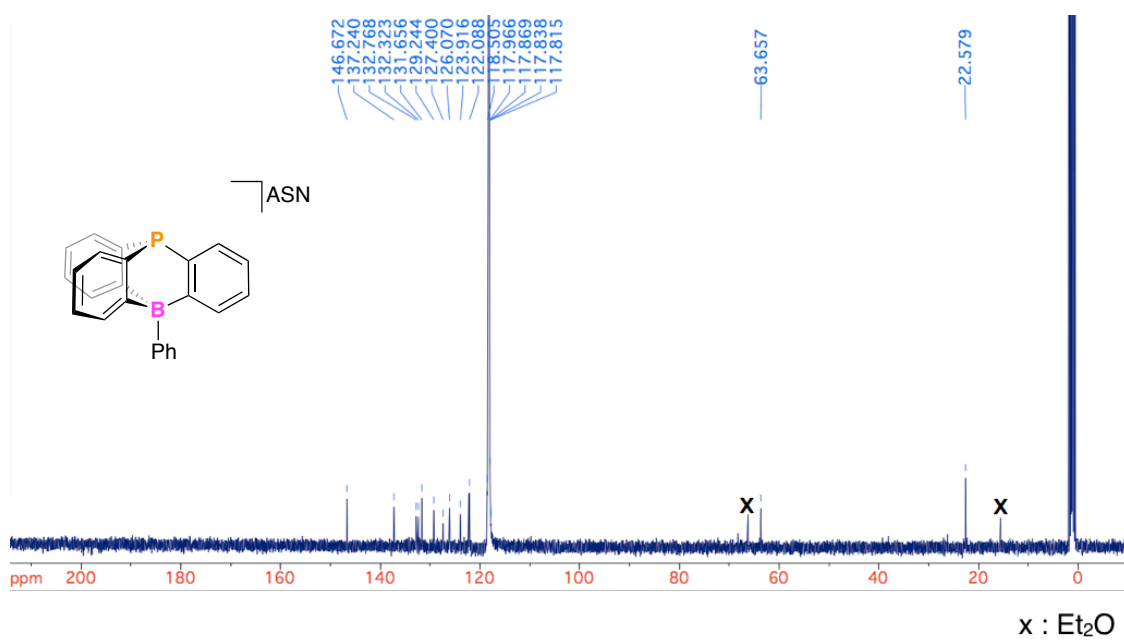
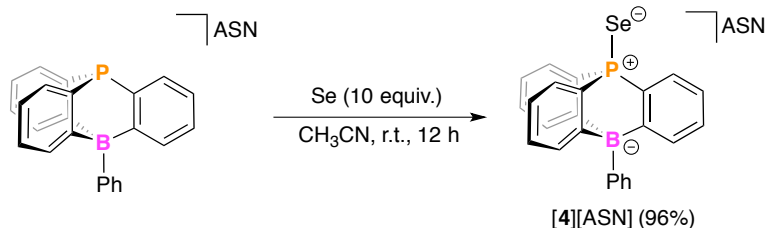


Figure S13. [3][ASN], $^{13}\text{C}\{^1\text{H}\}$ NMR, CD_3CN , 100 MHz, 298 K





5-azoniaspiro[4.4]nonane 9-phosphatriptycene-10-phenylborate selenide [4][ASN]: A mixture of [3][ASN] (10 mg, 0.021 mmol) and selenium powder (16.7 mg, 0.21 mmol) in CH_3CN (2 mL) was stirred for 24 h at room temperature. The excess of selenium in the reaction mixture was removed by filtration and the filtrate was evaporated to give the crude product, [4][ASN] as an off-white solid (11.3 mg, 96%). This solid was further recrystallized from Et_2O -layered CH_3CN solution at $-35\text{ }^\circ\text{C}$. Due to the low solubility of [4][ASN], a ^{13}C NMR spectrum was not collected.

^1H NMR (CD_3CN , 300 MHz, 298 K): δ = 8.02 (m, 3H), 7.97 (m, 2H; *o*-Ph), 7.49 (m, 2H), 7.44 (m, 3H), 7.26 (t, $^3J_{\text{H,H}}$ = 7.4 Hz, 1H; *p*-Ph), 6.99 (m, 6H), 3.32 (m, 2-H(ASN), 8H), 2.08 (m, 3-H(ASN), 8H).

$^{31}\text{P}\{^1\text{H}\}$ NMR (CD_3CN , 121 MHz, 298 K): δ = 11.15 (q, $^3J_{\text{P,B}}$ = 19.3 Hz with Se satellites, $^1J_{\text{P,Se}}$ = 746 Hz).

$^{11}\text{B}\{^1\text{H}\}$ NMR (CD_3CN , 128 MHz, 298 K): δ = -8.5 (d, $^3J_{\text{P,B}}$ = 19.3 Hz).

HR ESI(-)-MS: Calcd. 427.0326 for $\text{C}_{24}\text{H}_{17}\text{BPSe}$ [4] $^-$. Found. 427.0507 (with appropriate Se isotope pattern)

Figure S14. [4][ASN], ^1H NMR, CD_3CN , 300 MHz, 298 K (x = Et_2O)

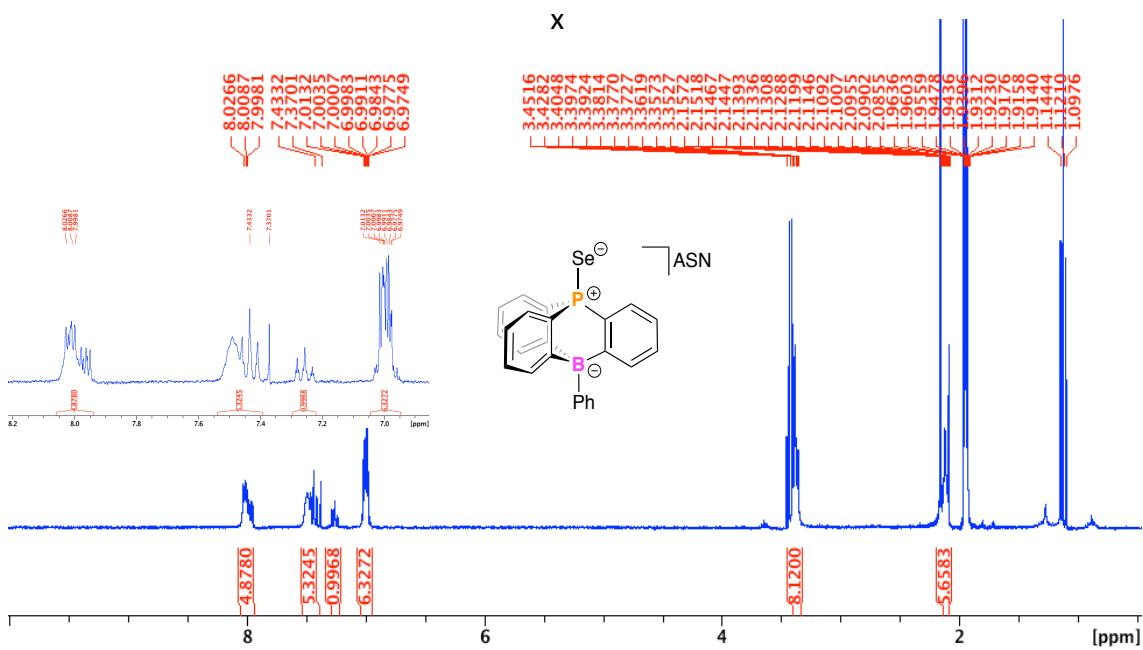
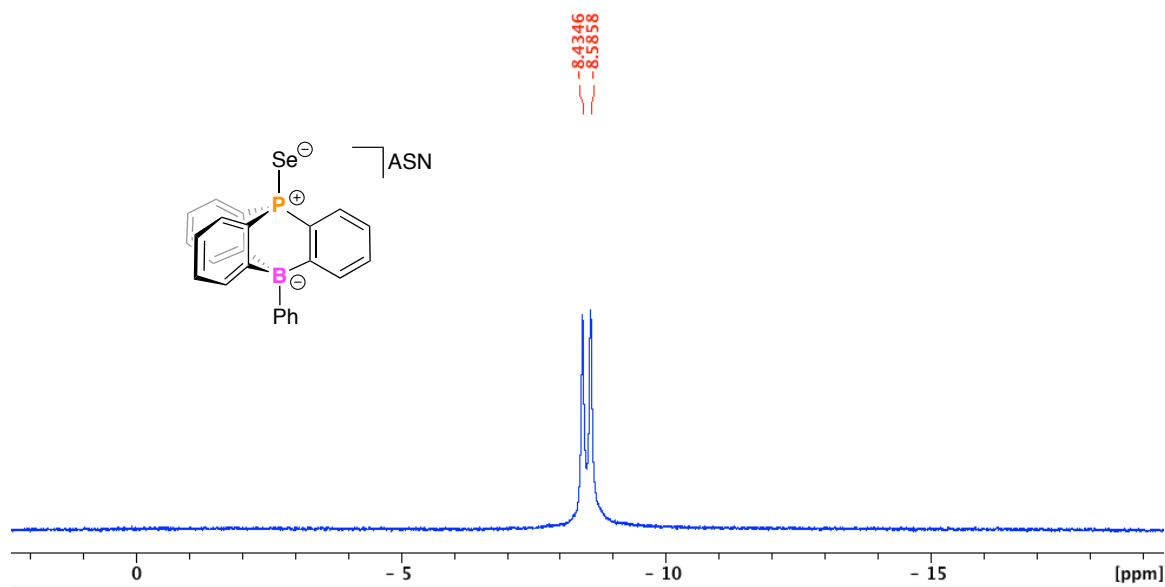
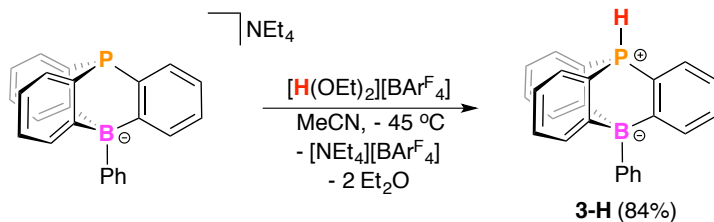


Figure S16. [4][ASN], $^{11}\text{B}\{^1\text{H}\}$ NMR, CD_3CN , 128 MHz, 298 K





Hydrogen 9-phosphatriptycene-10-phenylborate (**3-H**): To an CH₃CN solution (1 mL) of [3][NEt₄] (10 mg, 0.021 mmol) at -35 °C was added [H-OEt₂][BARF₄] (21.2 mg, 0.21 mmol) in one portion. The reaction mixture was warmed to room temperature and allowed to stir for 1 h after which time all volatiles were removed *in-vacuo*. Next, the white residue was washed with toluene (40 mL) and filtered through a Celite[®] plug. Combination of the toluene extracts and removal of volatiles *in-vacuo* afforded **3-H** as a white solid (6.1 mg, 84%).

¹H NMR (CD₃CN, 400 MHz, 298 K): δ = 8.49 (d, ¹J_{P,H} = 512 Hz, 1H), 7.97 (br, 2H), 7.85 (br, 3H), 7.61 (br, 3H), 7.46 (t, ³J_{H,H} = 7.2 Hz, 2H), 7.30 (br, 1H), 7.19 (br, 3H), 7.06 (br, 3H).

³¹P{¹H} NMR (CD₃CN, 162 MHz, 298 K): δ = -25.3 (d, ¹J_{P,H} = 512 Hz)

¹¹B{¹H} NMR (CD₃CN, 128 MHz, 298 K): δ = -9.1 (d, ³J_{P,B} = 23.1 Hz).

Figure S17. 3-H, ^1H NMR, CD_3CN , 400 MHz, 298 K (x = toluene)

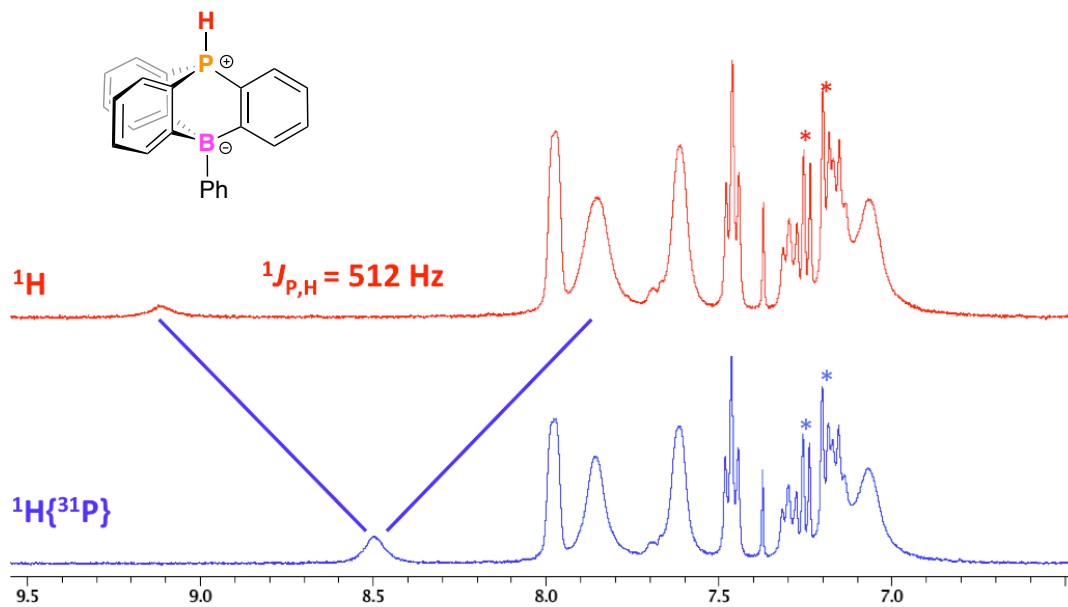
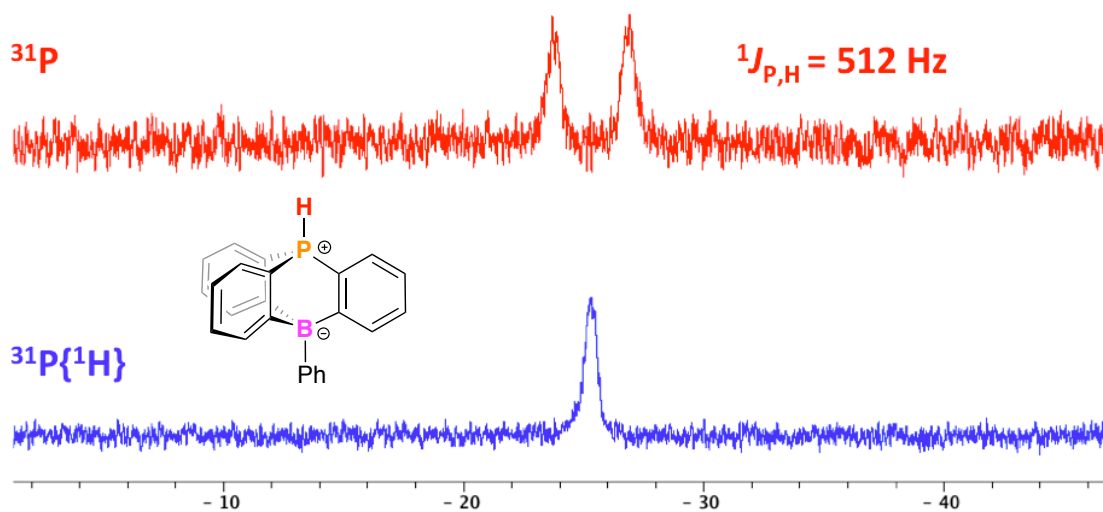
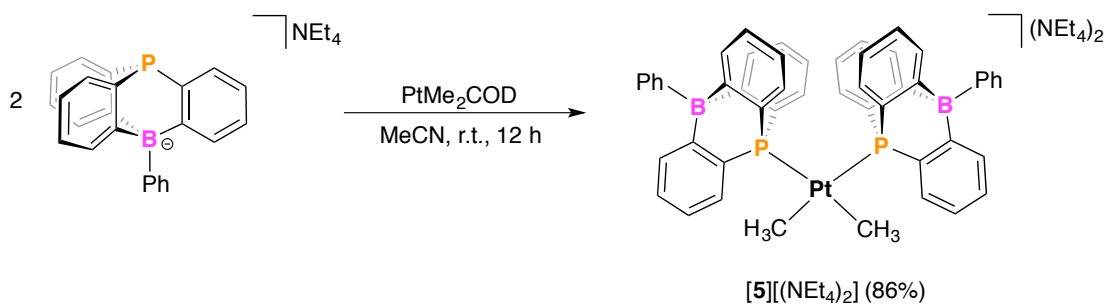


Figure S18. 3-H, ^{31}P NMR, CD_3CN , 162 MHz, 298 K





cis-[PtMe₂[3]₂][NEt₄]₂ ([5][NEt₄]₂): A solution of PtMe₂(cod) (10.5 mg, 31.5 μmol) and [3][NEt₄] (30 mg, 62.9 μmol) were combined in CH₃CN (4 mL) and stirred for 12 h at ambient temperature to give a clear colorless solution. Removal of solvents *in-vacuo* and washing the residue with hexane gave the crude product, [5][NEt₄]₂ as a white solid (32 mg, 86%).

¹H NMR (THF-*d*₈, 400 MHz, 298 K): δ = 7.91 (dd, ³J_{H,H} = 7.2 Hz, 6H), 8.07 (br, 4H; *o*-Ph), 7.41 (m, 10H), 7.22 (t, ³J_{H,H} = 7.3 Hz, 2H; *p*-Ph), 6.72 (t, ³J_{H,H} = 7.8 Hz, 6H), 6.46 (t, ³J_{H,H} = 7.3 Hz, 6H), 3.15 (q, ³J_{H,H} = 7.1 Hz, 8H; CH₂(NEt₄)), 1.13 (t, ³J_{H,H} = 7.1 Hz, 12H; CH₂(NEt₄)), 0.88 (t, Pt-CH₃, ³J_{H,P} = 6.1 Hz with ²J_{H,Pt} = 69.6 Hz satellites, 6H).

³¹P{¹H} NMR (CD₃CN, 162 MHz, 298 K): δ = -1.29 (Pt satellites, ¹J_{P,Pt} = 2672 Hz).

¹¹B{¹H} NMR (THF-*d*₈, 128.3 MHz, 298 K): δ = -6.8 (d, ³J_{P,B} = 4 Hz).

¹³C NMR (THF-*d*₈, 101 MHz, 298 K): δ = 169.3 (virtual quintet, *J* ~ 40 Hz), 142.9 (d, *J* = 45.5 Hz), 137.5, 134.1 (virtual quintet, *J* = 24.5 Hz), 130.4, 126.4, 124.4, 122.6, 120.2 (d, *J* = 11.6 Hz), 58.2, 46.0, 7.83 (dd, ²J_{C,P} = 91 Hz, ²J_{C,P} = 11 Hz with Pt satellites, ¹J_{C,Pt} = 597 Hz).

HR ESI(-)-MS: Calcd. 904.220 for [M-CH₃]⁻. Found. 904.214, Calcd. 945.247 for [M-CH₃ + NCCH₃]⁻. Found. 945.240 (with appropriate Pt isotope pattern).

Anal. Calc. for C₆₆H₈₀B₂N₂P₂Pt: C, 67.18; H, 6.83; N, 2.37. Found: C, 65.02; H, 6.48; N, 2.65.

Figure S19. [5][NEt₄]₂, ¹H NMR, THF-*d*₈, 400 MHz, 298 K

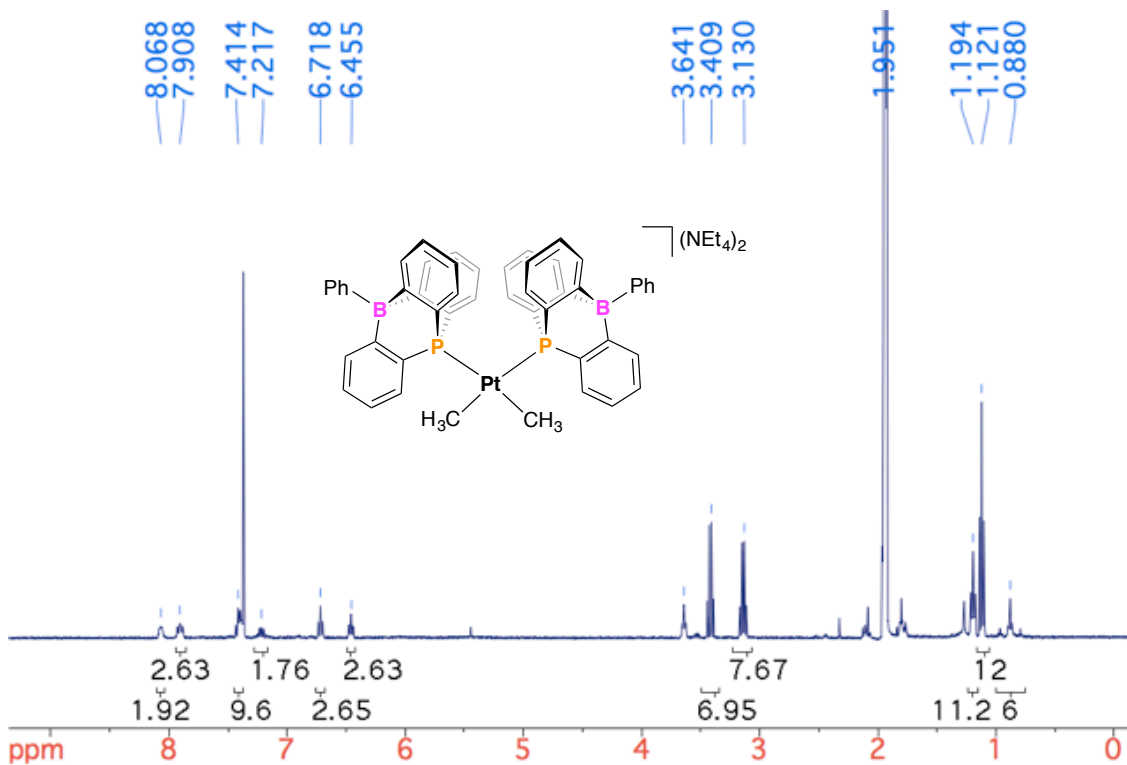


Figure S20. [5][NEt₄]₂, ³¹P{¹H} NMR (CD₃CN, left) and ¹¹B{¹H} NMR (THF-*d*₈, right), 298 K

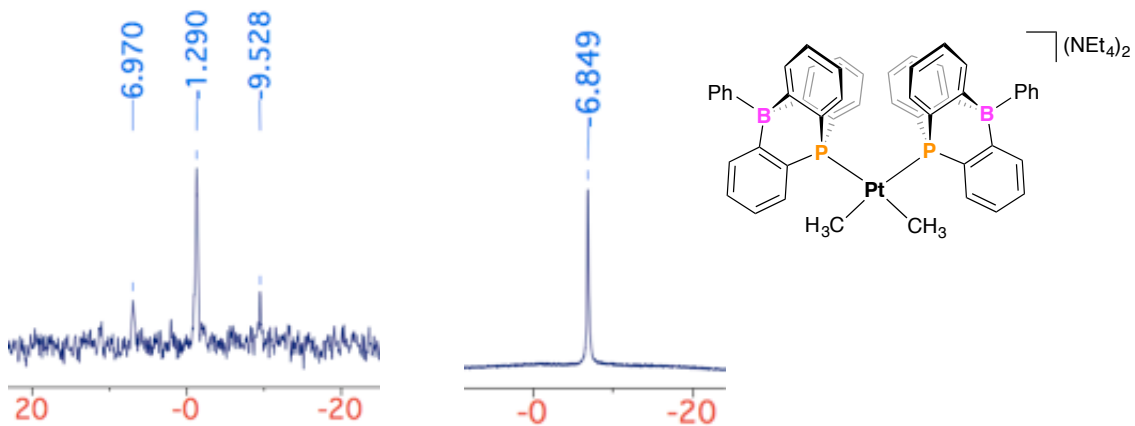
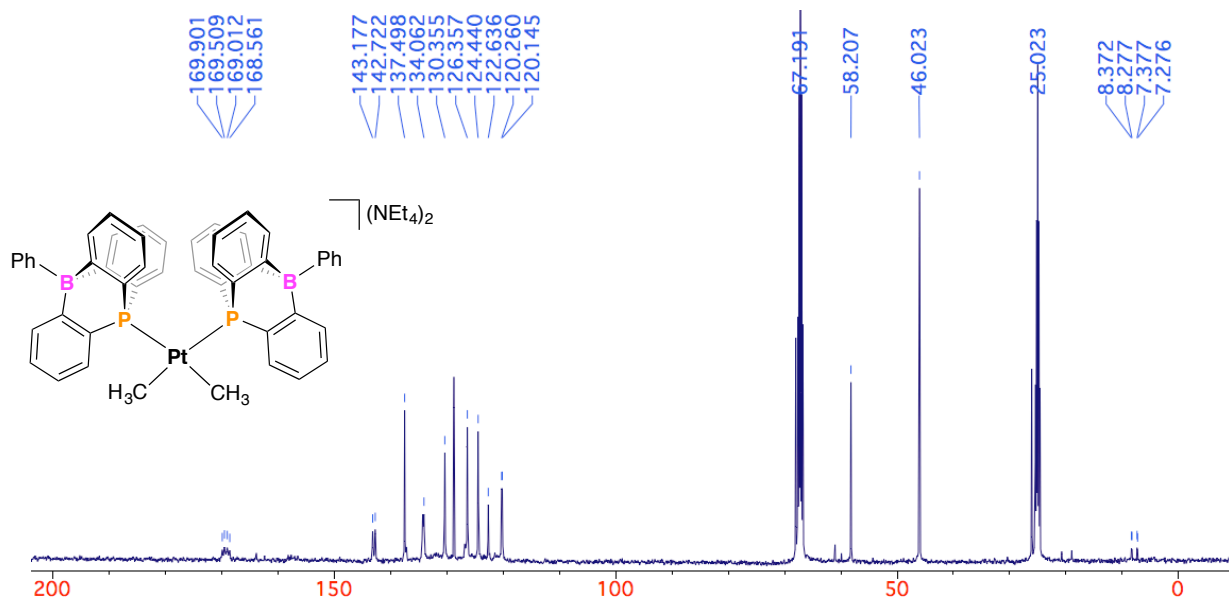
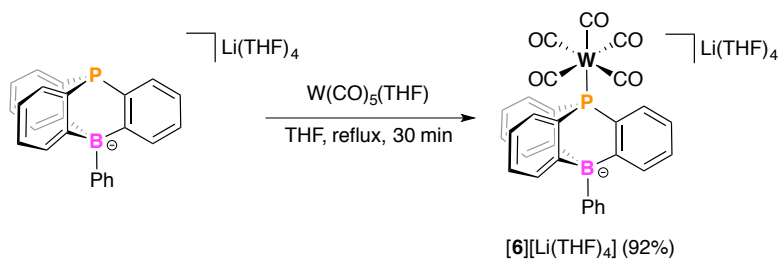


Figure S21. [5][NEt₄]₂, ¹³C{¹H} NMR, THF-d₈, 100 MHz, 298 K





[WCO₅[3]][Li(THF)₄] (**[6][Li(THF)₄]**): A mixture of **[3][Li(THF)₄]** (61 mg, 94.2 μmol) and **[WCO₅(THF)]** (33 mg, 94.2 μmol) in THF (4 mL) was stirred for 30 min under reflux. The solvents were evaporated, and the residue was washed with toluene and filtered giving **[6][Li(THF)₄]** as a yellow solid (84 mg, 92%).

¹H NMR (C₆D₆, 400 MHz, 298 K): δ = 8.51 (d, ³ $J_{\text{H,H}}$ = 8.0 Hz, 3H), 8.36 (dd, ³ $J_{\text{H,H}}$ = 6.4 Hz, ³ $J_{\text{H,H}}$ = 8.0 Hz, 2H), 8.07 (d, ³ $J_{\text{H,H}}$ = 6.4 Hz, 2H), 7.69 (t, ³ $J_{\text{H,H}}$ = 7.6 Hz, 3H), 7.50 (t, ³ $J_{\text{H,H}}$ = 7.6 Hz, 3H), 6.94 (br, 4H), 3.45 (m, 16H; THF), 1.34 (m, 16H; THF).

⁷Li{¹H} NMR (C₆D₆, 156 MHz, 298 K): δ = -1.57.

³¹P{¹H} NMR (C₆D₆, 162 MHz, 298 K): δ = -5.1.

¹¹B{¹H} NMR (C₆D₆, 128 MHz, 298 K): δ = -8.51.

IR (THF, 298 K, cm⁻¹): ν = 2064, 2004, 1943 (ν_{CO}). *c.f.* ν_{CO} = 2074, 1988, 1946 for Ph₃PW(CO)₅.⁴

Figure S22. [6][Li(THF)₄], ¹H NMR, C₆D₆, 400 MHz, 298 K

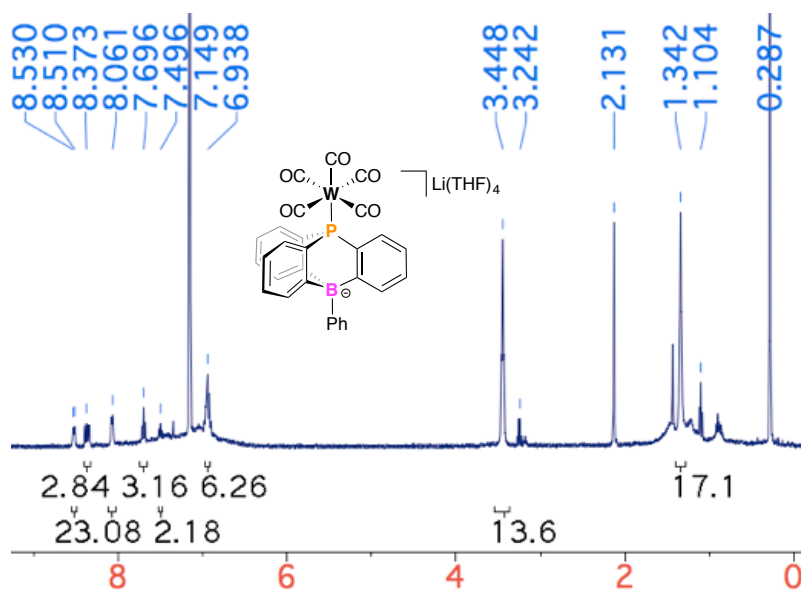


Figure S23. [6][Li(THF)₄], ⁷Li{¹H} NMR, C₆D₆, 156 MHz, 298 K

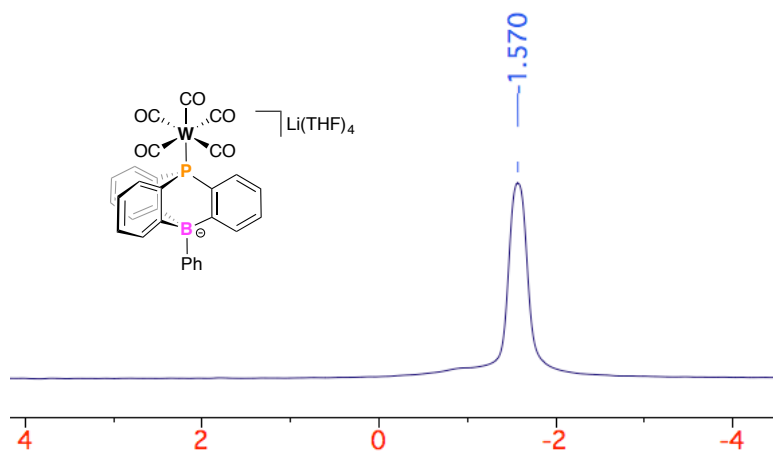


Figure S24. [6][Li(THF)₄], ³¹P{¹H} NMR, C₆D₆, 162 MHz, 298 K

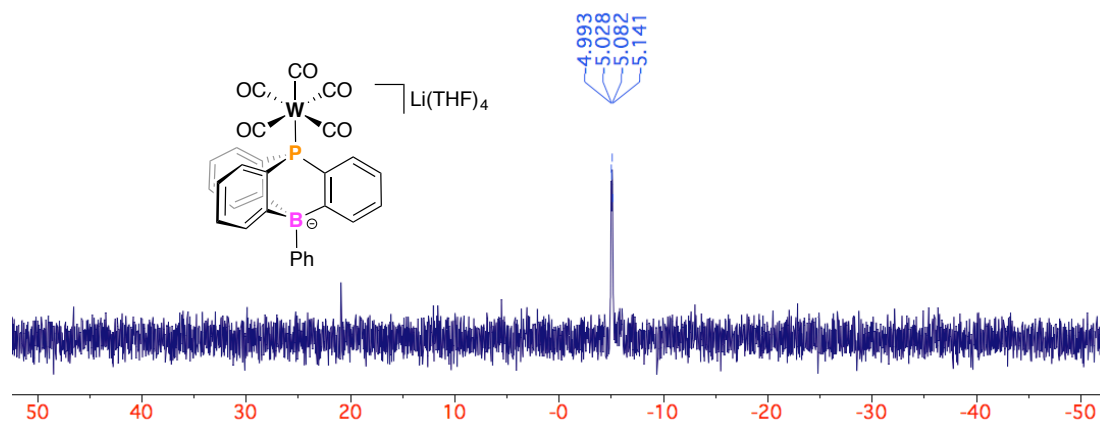
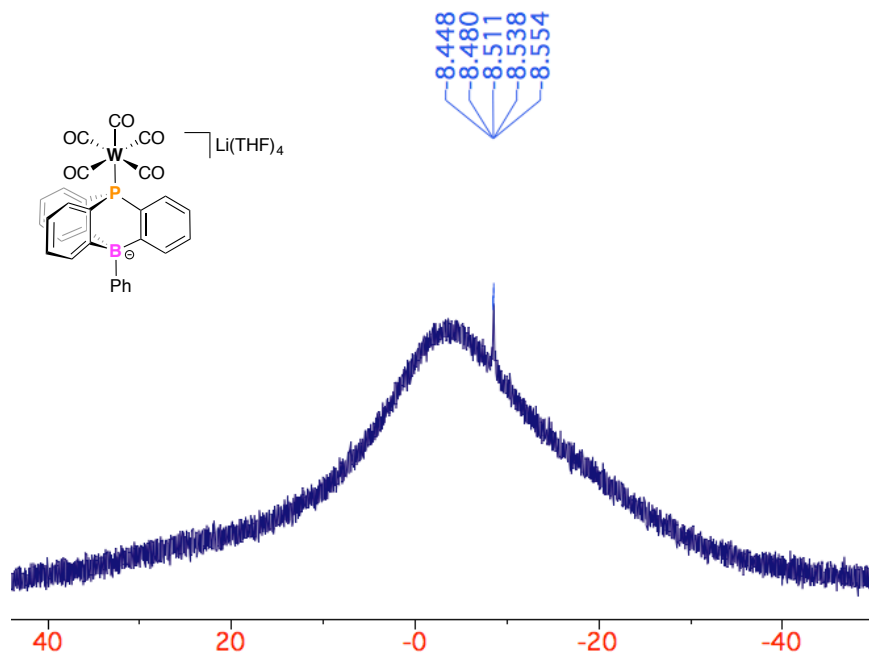
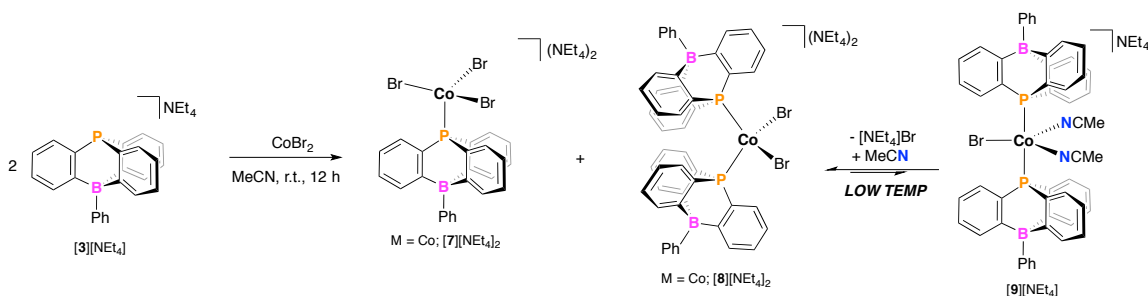


Figure S25. [6][Li(THF)₄], ¹¹B{¹H} NMR, C₆D₆, 128 MHz, 298 K





[7][NEt₄]₂, [8][NEt₄]₂, and [9][NEt₄]₂: A mixture of [3][NEt₄] (30 mg, 62.9 μmol) and CoBr₂ (7 mg, 32.1 μmol) in CH₃CN (4 mL) was stirred for 12 h at ambient temperature. Next, the solvent was removed *in-vacuo* and the resulting material washed with toluene to give a turquoise solid (35 mg, 95% by mass). Cooling of a CH₃CN solution of this sample at -35 °C resulted in the formation of a forest green solution. Layering this solution with Et₂O or THF gave blue, green, and turquoise blocks (Figure S26) suitable for analysis by single crystal X-ray diffraction.

¹H NMR (CD₃CN, 400 MHz, 298 K): δ = 27.10 (br), 22.68, 19.40 (br), 7.81, 7.25, 7.09, 6.99, 6.51, 5.77, 5.54, 5.06, 4.31, 3.42 (NEt₄), 3.08 (NEt₄), 1.22 (NEt₄), 1.20 (NEt₄).

UV-VIS (MeCN, 0.6 mg/mL, 1 cm cell, 298 K): 617, 642, 668, 681, and 696 nm.

UV-VIS (MeCN, 0.6 mg/mL, 1 cm cell, 233 K): 310 (*new*), 376 (*new*), 617, 642, 668, 681, and 696 nm.

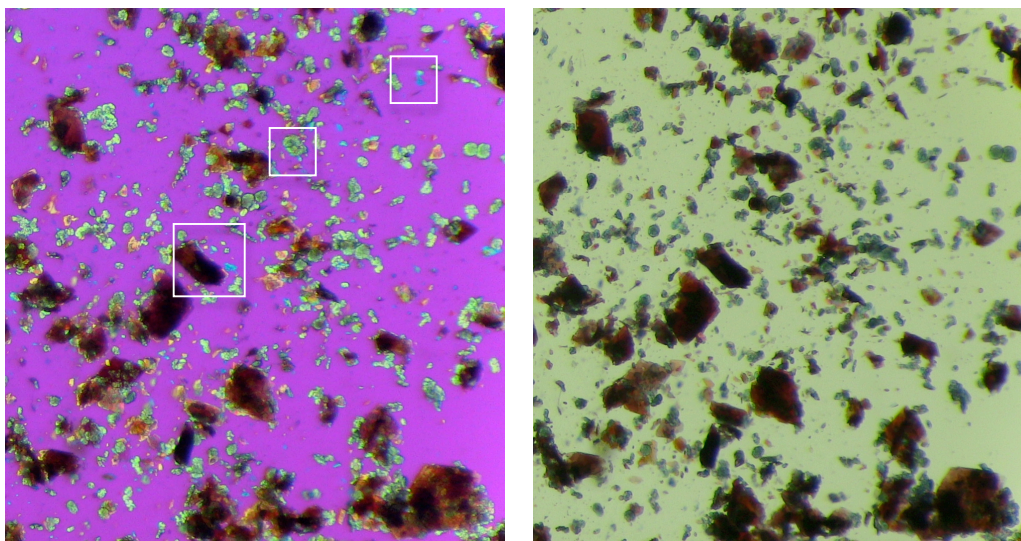
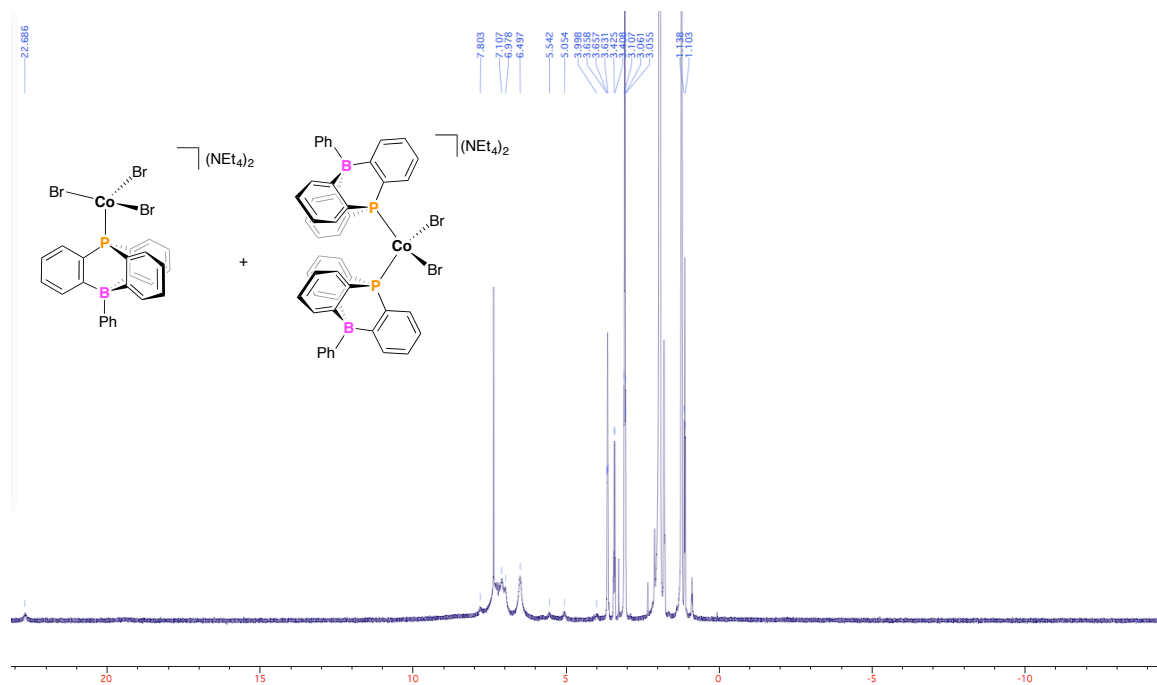
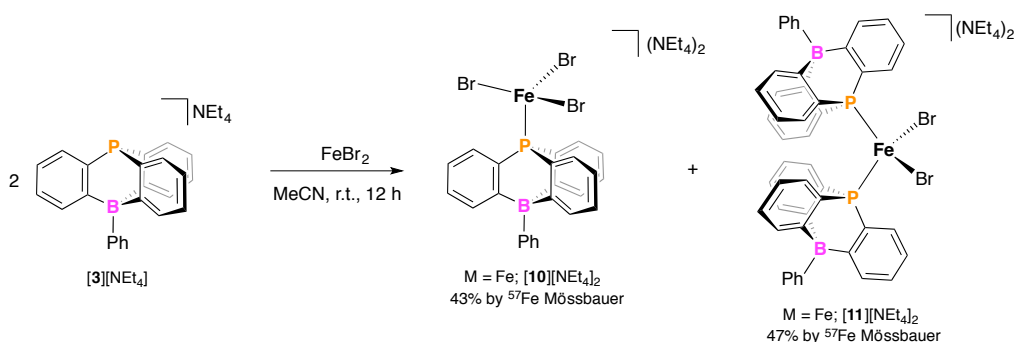


Figure S26. Microscope image of single crystals grown from the above reaction mixture. Left panel (polarizer), right panel (no polarizer).

Figure S27. Reaction between 2 equiv. [3][NEt₄] and CoBr₂, ¹H NMR, CD₃CN, 400 MHz, 298 K





$[10][NEt_4]_2$ and $[11][NEt_4]_2$: A mixture of $[3][NEt_4]$ (30 mg, 62.9 μ mol) and $FeBr_2$ (7 mg, 32.1 μ mol) in CH_3CN (4 mL) was stirred for 12 h at ambient temperature. Next, the solvent was removed *in-vacuo* and the resulting material washed with toluene to give a beige solid (33 mg, 89% by mass). On the basis of 80 K ^{57}Fe Mössbauer spectroscopy of a frozen CH_3CN solution of this solid, three Fe-containing species were identified: $[Fe(PTB)Br_3][NEt_4]_2$ (43%, $[10][NEt_4]_2$), $[Fe(PTB)_2Br_2][NEt_4]_2$ (47%, $[11][NEt_4]_2$), and a higher coordinate Fe species (10%).

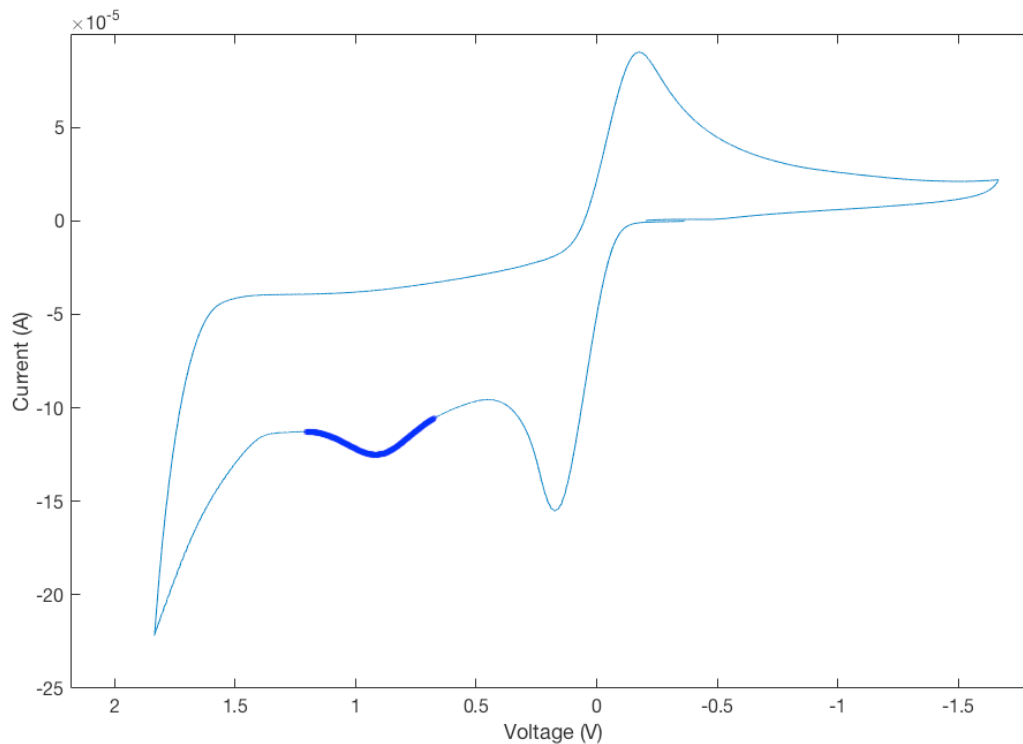
1H NMR (CD_3CN , 400 MHz, 298 K): $\delta = 29.12$ (br), 13.05, 6.99, 3.42, 3.02 (NEt_4), 1.09 (NEt_4), -6.4 (br).

^{57}Fe Mössbauer (80 K, MeCN solution, mm/s): $\delta = 0.87$; $\Delta E_Q = 2.34$ (43%, $[10][NEt_4]_2$), $\delta = 0.79$; $\Delta E_Q = 2.87$ (47%, $[11][NEt_4]_2$), $\delta = 1.72$; $\Delta E_Q = 2.52$ (10%, unknown)

Electrochemical Details:

Cyclic voltammetry (CV) measurements were carried out in a glovebox under an N₂ atmosphere in a one-compartment cell using a CH Instruments 600B electrochemical analyzer. A glassy carbon electrode was used as the working electrode and a carbon rod was used as the auxiliary electrode. The reference electrode was AgOTf/Ag in THF isolated by a CoralPor™ frit (obtained from BASi). The ferrocenium/ferrocene couple (Fc⁺/Fc) was used as an external reference. THF solutions of electrolyte (0.1 M [NBu₄][ClO₄]) and analyte (1 mM) were also prepared under an inert atmosphere.

Figure S29. [3][NEt₄], CV, CH₂Cl₂, 298 K showing an irreversible oxidative feature at 0.97 V (highlighted in blue). The ferrocenium/ferrocene reference couple (Fc⁺/Fc) is shown at 0 V.



Crystallographic details:

All crystals were mounted on a glass fiber loop. All measurements were made using graphite-monochromated Mo K α ($\lambda=0.71073$ Å) or Cu K α ($\lambda=1.54178$ Å) radiation on a Bruker AXS D8 VENTURE KAPPA diffractometer coupled to a PHOTON 100 CMOS detector. The structures were solved by direct methods⁵ and refined by full-matrix least-squares procedures on F2 (SHELXL-2013)⁵ using the OLEX2 interface.⁶ All hydrogen atoms were placed in calculated positions. Non-hydrogen atoms were refined anisotropically.

Additional details:

[4][ASN]: This crystal is an inversion twin – the following law, obtained by OLEX2, was employed: **TWIN** (-1 0 0 0 1 0 0 0 -1 2), **BASF** 0.581.

[5][NEt₄]₂: This crystal contained electron density assignable to disordered solvent. OLEX2 was used to identify voids and a solvent mask was applied [two void volumes = 476 Å³ corresponding to 142.3 electrons each]. The ADP of C33 was restrained using ISOR to be approximately isotropic and enhanced rigid bond restraints were employed using RIGU (across the entire molecule). These applications gave a good improvement of data statistics.

[7][NEt₄]₂: This crystal is a twin – the following law, obtained by OLEX2, was employed: **TWIN** (-1 0 0 0 -1 0 0.272 0 1 2), **BASF** 0.294. The ADP of C1 and C21 were restrained using ISOR to be approximately isotropic and enhanced rigid bond restraints were employed using RIGU (across the entire molecule). *N.B.* The data obtained were of low quality due to poor crystal quality.

[8][NEt₄][Na(THF)₄(NCMe)₂]: The ADP of O1, C49, C50, C51, C52, C69, C70, C71, and C72 were restrained using ISOR to be approximately isotropic and enhanced rigid bond restraints were employed using RIGU (across the entire molecule). The Na centre of the Na(THF)₄(NCMe)₂⁺ counterion was modelled as a Co atom having occupancy 1 (XTAL 0.5). These applications gave a good improvement of data statistics.

[9][NEt₄]: The data obtained were of very low quality due to poor crystal quality and are reported to establish bulk connectivity, thus *metrics taken from this dataset should be used with caution*. The ADP of C26, C28, N5, N6, and C33 were restrained using ISOR to be approximately isotropic and enhanced rigid bond restraints were employed using RIGU (across the entire molecule).

CCDC **1824471-1824478** contains the supplementary crystallographic data for this paper. These data can be obtained free of charge from The Cambridge Crystallographic Data Centre *via* www.ccdc.cam.ac.uk/data_request/cif

Table S1. Crystallographic data for [3][NEt₄], [3][ASN], [4][ASN], and [5][NEt₄]₂

Compound	[3][NEt ₄]	[3][ASN]	[4][ASN]	[5][NEt ₄] ₂
Empirical formula	C ₆₄ H ₇₄ B ₂ N ₂ P ₂	C ₃₆ H ₄₁ BNOP	C ₃₂ H ₃₃ BNPSe	C ₆₆ H ₈₀ B ₂ N ₂ P ₂ Pt
Formula weight	954.81	545.48	552.33	1179.97
Temperature/K	100(2)	100(2)	100(2)	100(2)
Crystal system	Monoclinic	Monoclinic	Orthorhombic	Orthorhombic
Space group	<i>P2₁/c</i>	<i>P2₁/n</i>	<i>Pca2₁</i>	<i>Pbcn</i>
a/Å	18.893(2)	10.0854(10)	17.601(3)	16.7080(8)
b/Å	15.0154(15)	17.8383(16)	17.365(2)	22.4099(11)
c/Å	20.461(2)	16.1920(16)	17.358(2)	16.7415(8)
α/°	90	90	90	90
β/°	114.845(4)	96.009(4)	90	90
γ/°	90	90	90	90
V/Å ³	5267.4(9)	2897.0(5)	5305.3(13)	6268.4(5)
Z	4	4	8	4
ρ/ g/cm ⁻³	1.204	1.251	1.383	1.250
μ/ mm ⁻¹	0.126	0.125	1.498	2.328
F(000)	2048.0	1168.0	2288.0	2432.0
Crystal size/ mm ³	0.32 × 0.29 × 0.15	0.35 × 0.27 × 0.15	0.15 × 0.14 × 0.057	0.19 × 0.18 × 0.02
Radiation	MoKα (λ = 0.71073)	MoKα (λ = 0.71073)	MoKα (λ = 0.71073)	MoKα (λ = 0.71073)
2θ range for data collection/°	4.712 to 55.008	4.554 to 55.004	4.628 to 68.808	4.866 to 55.024
Index ranges	-24 ≤ h ≤ 24, -19 ≤ k ≤ 19, -26 ≤ l ≤ 26	-13 ≤ h ≤ 13, -23 ≤ k ≤ 23, -21 ≤ l ≤ 21	-27 ≤ h ≤ 26, -27 ≤ k ≤ 27, -27 ≤ l ≤ 26	-21 ≤ h ≤ 21, -29 ≤ k ≤ 28, -21 ≤ l ≤ 21
Independent reflections	12103 [R _{int} = 0.0798, R _{sigma} = 0.0278]	6642 [R _{int} = 0.0800, R _{sigma} = 0.0268]	22073 [R _{int} = 0.1514, R _{sigma} = 0.0685]	7201 [R _{int} = 0.1159, R _{sigma} = 0.0517]
Data/restraints/parameters	12103/0/639	6642/0/361	22073/1/650	7201/312/335
Goodness-of-fit on F ²	1.043	1.065	1.024	1.085
R [I ≥ 2θ (I)] (R1, wR2)	R ₁ = 0.0427, wR ₂ = 0.1243	R ₁ = 0.0409, wR ₂ = 0.1121	R ₁ = 0.0453, wR ₂ = 0.1086	R ₁ = 0.0735, wR ₂ = 0.1530
R (all data) (R1, wR2)	R ₁ = 0.0556, wR ₂ = 0.1333	R ₁ = 0.0530, wR ₂ = 0.1214	R ₁ = 0.0588, wR ₂ = 0.1133	R ₁ = 0.1027, wR ₂ = 0.1630
Largest diff. peak/hole / (e Å ⁻³)	0.86/-0.37	1.39/-0.31	1.41/-0.72	5.63/-2.34

$$R1 = \sum ||F_o| - |F_c|| / \sum |F_o|; wR2 = [\sum (w(F_o^2 - F_c^2)^2) / \sum w(F_o^2)^2]^{1/2}$$

Table S2. Crystallographic data for [7][NEt₄]₂, [8][NEt₄][Na(THF)₄(NCMe)₂], [9][NEt₄], and [10][NEt₄]₂

Compound	[7][NEt ₄] ₂	[8][NEt ₄][Na(THF) ₄ (NCMe) ₂]	[9][NEt ₄]**	[10][NEt ₄] ₂
Empirical formula	C ₄₀ H ₅₇ BBr ₃ CoN ₂ P	C ₁₄₄ H ₁₆₈ B ₄ Br ₄ Co ₃ N ₆ O ₆ P ₄	C ₇₀ H ₇₅ B ₂ BrCoN ₈ P ₂	C ₄₀ H ₅₇ BBr ₃ FeN ₂ P
Formula weight	906.31	2742.38	1268.92	903.23
Temperature/K	100(2)	100(2)	100(2)	100(2)
Crystal system	Monoclinic	Monoclinic	Orthorhombic	Monoclinic
Space group	<i>P</i> 2 ₁ / <i>n</i>	<i>P</i> 2 ₁ / <i>c</i>	<i>Cmce</i>	<i>P</i> 2 ₁ / <i>n</i>
<i>a</i> /Å	13.5630(10)	22.776(2)	25.9634(18)	13.5457(11)
<i>b</i> /Å	16.1347(13)	11.6346(12)	17.7060(13)	16.1351(13)
<i>c</i> /Å	18.6380(16)	27.261(3)	29.773(2)	18.6839(15)
α /°	90	90	90	90
β /°	95.679(4)	113.332(3)	90	95.303(4)
γ /°	90	90	90	90
<i>V</i> /Å ³	4058.6(6)	6633.1(12)	13686.8(17)	4066.1(6)
<i>Z</i>	4	2	8	4
ρ / g/cm ⁻³	1.483	1.373	1.232	1.475
μ / mm ⁻¹	7.362	1.682	3.436	3.388
<i>F</i> (000)	1852.0	2846.0	5368.0	1848.0
Crystal size/ mm ³	0.21 × 0.18 × 0.14	0.24 × 0.18 × 0.07	0.21 × 0.18 × 0.12	0.44 × 0.41 × 0.27
Radiation	CuK α (λ = 1.54178)	MoK α (λ = 0.71073)	CuK α (λ = 1.54178)	MoK α (λ = 0.71073)
2 θ range for data collection/°	4.764 to 159.868	4.406 to 55.016	5.936 to 112.964	4.638 to 58.386
Index ranges	-16 ≤ <i>h</i> ≤ 17, -20 ≤ <i>k</i> ≤ 20, -23 ≤ <i>l</i> ≤ 22	-29 ≤ <i>h</i> ≤ 29, -15 ≤ <i>k</i> ≤ 15, -35 ≤ <i>l</i> ≤ 35	-28 ≤ <i>h</i> ≤ 27, -19 ≤ <i>k</i> ≤ 19, -31 ≤ <i>l</i> ≤ 32	-18 ≤ <i>h</i> ≤ 18, -22 ≤ <i>k</i> ≤ 22, -25 ≤ <i>l</i> ≤ 25
Independent reflections	8674 [R _{int} = 0.0856, R _{sigma} = 0.0510]	15217 [R _{int} = 0.1050, R _{sigma} = 0.0527]	4624 [R _{int} = 0.3423, R _{sigma} = 0.1213]	10966 [R _{int} = 0.0578, R _{sigma} = 0.0201]
Data/restraints/parameters	8674/393/443	15217/765/769	4624/375/404	10966/0/441
Goodness-of-fit on <i>F</i> ²	2.068	1.004	1.053	1.044
R [<i>I</i> ≥ 2 θ (<i>I</i>)] (R1, wR2)	R ₁ = 0.1602, wR ₂ = 0.4098	R ₁ = 0.0610, wR ₂ = 0.1377	R ₁ = 0.1730, wR ₂ = 0.4104	R ₁ = 0.0340, wR ₂ = 0.0841
R (all data) (R1, wR2)	R ₁ = 0.1737, wR ₂ = 0.4362	R ₁ = 0.0946, wR ₂ = 0.1536	R ₁ = 0.2300, wR ₂ = 0.4570	R ₁ = 0.0432, wR ₂ = 0.0885
Largest diff. peak/hole / (e Å ⁻³)	4.82/-1.39	2.77/-1.20	1.44/-1.13	1.95/-1.06

$$R1 = \frac{\sum ||F_o| - |F_c||}{\sum |F_o|}; wR2 = \frac{[\sum (w(F_o^2 - F_c^2)^2)]}{\sum w(F_o^2)^2}]^{1/2}$$

** The data obtained were of very low quality due to poor crystal quality and are reported to establish net connectivity.

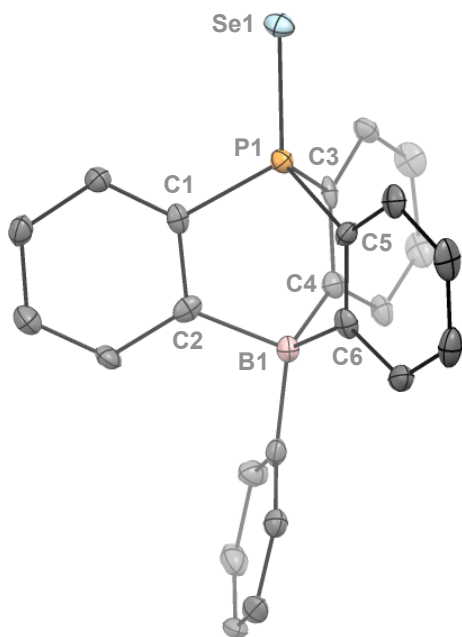


Figure S30. ORTEP depiction of the solid-state molecular structure of [4][ASN] (displacement ellipsoids are shown at the 50% probability, hydrogens and ASN^+ counterion omitted for clarity). Selected bond lengths [\AA] and angles ($^\circ$). P(1)-C(1) 1.793(4), P(1)-C(3) 1.812(4), P(1)-C(5) 1.801(4), B(1)-C(2) 1.648(2), B(1)-C(4) 1.652(7), B(1)-C(6) 1.658(6), B(1)-P(1) 2.911(5), P(1)-Se(1) 2.108(1), $\angle\text{C-P(1)-C}$ 100.6 (avg.), $\angle\text{C-B(1)-C}$ 104.5 (avg.), $\Sigma(\text{C-P-C})$ 301.8.

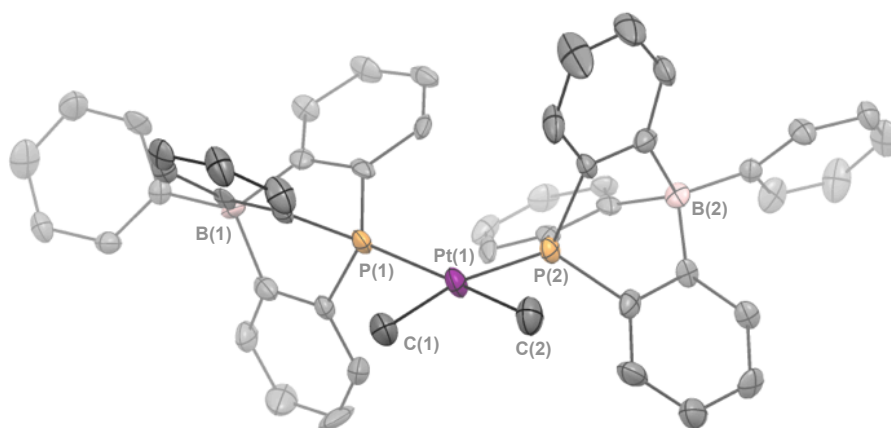


Figure S31. ORTEP depiction of the solid-state molecular structure of [5][NEt_4]₂ (displacement ellipsoids are shown at the 50% probability, counterions and hydrogens omitted for clarity). Selected bond lengths [\AA] and angles ($^\circ$): Pt(1)-P(1) 2.2926(18), Pt(1)-C(1) 2.107(8), B(1)-P(1) 2.985(8), $\angle\text{C(1)-Pt(1)-C(2)}$ 81.6(5), P(1)-Pt(1)-P(2) 103.00(9), $\angle\text{C(1)-Pt(1)-P(1)}$ 88.1(2).

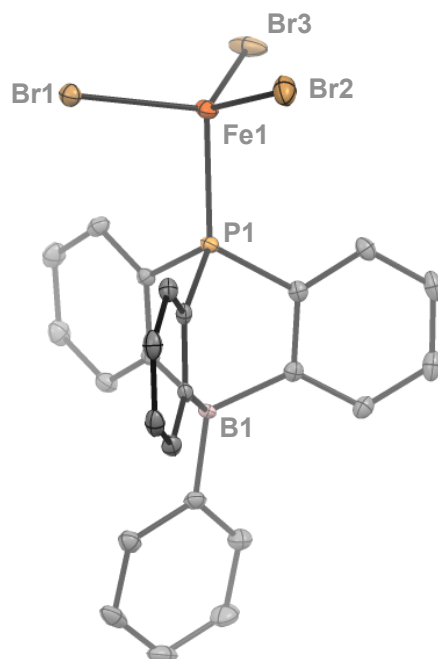


Figure S32. ORTEP depiction of the solid-state molecular structure of **[10][NEt₄]₂** (displacement ellipsoids are shown at the 50% probability, hydrogens and counterion omitted for clarity). Selected bond lengths [Å] and angles (°). Fe(1)-P(1) 2.4320(6), Fe(1)-Br(1) 2.4098(5), Fe(1)-Br(2) 2.4212(5), Fe(1)-Br(3) 2.4514(5), P(1)-B(1) 2.964(2), P(1)-Fe(1)-Br(1) 102.03(2), P(1)-Fe(1)-Br(2) 100.51(2), P(1)-Fe(1)-Br(3) 109.20(2).

DFT Calculations:

Geometry optimization of [3]⁻ was performed using Gaussian 09 [Rev. A.02]⁷ at the following level of theory: B3LYP/6-311G(d) for P and 6-31G(d) for all other atoms. A frequency calculation was performed on the optimized geometry to ensure a true minimum.

Table S3. Optimized Coordinates for [3]⁻

P	-2.501124	0.619195	-0.000841
C	-1.791251	-0.412989	1.367178
C	-0.422738	-0.773006	1.282784
C	-2.622099	-0.885676	2.387261
C	0.034547	-1.687485	2.24648
C	-2.120778	-1.759819	3.356983
H	-3.667387	-0.580594	2.415167
C	-0.79139	-2.170539	3.269371
H	1.057476	-2.050522	2.196501
H	-2.764838	-2.128648	4.153531
H	-0.390619	-2.876161	3.99661
C	-1.791067	-0.415918	-1.366536
C	-2.621811	-0.890834	-2.385676
C	-0.422558	-0.775743	-1.281222
C	-2.12039	-1.767087	-3.35344
H	-3.667091	-0.585802	-2.41436
C	0.034806	-1.692358	-2.242855
C	-0.791027	-2.177653	-3.264763
H	-2.764368	-2.137663	-4.149244
H	1.057735	-2.05528	-2.191994
H	-0.390188	-2.884889	-3.990398
C	-1.195812	1.919189	-0.002079
C	0.145465	1.477675	-0.001509
C	-1.532457	3.277248	-0.003443
C	1.132516	2.477881	-0.002398
C	-0.527048	4.247682	-0.004318
H	-2.580705	3.573825	-0.003834
C	0.807644	3.839041	-0.003769
H	2.180938	2.190291	-0.001982
H	-0.782614	5.306124	-0.005414
H	1.60347	4.583362	-0.004429
B	0.430369	-0.154785	0.000187
C	2.049458	-0.402272	0.00053
C	2.810551	-0.42456	1.190035
C	2.810506	-0.426667	-1.188976
C	4.204934	-0.52595	1.20037
H	2.298044	-0.336304	2.143904
C	4.204884	-0.528076	-1.199194
H	2.29794	-0.34012	-2.142962
C	4.915278	-0.592903	0.000636
H	4.737748	-0.54349	2.150554
H	4.737664	-0.547296	-2.149364
H	6.000836	-0.675919	0.000689

References:

- (1) Tsuji, H.; Inoue, T.; Kaneta, Y.; Sase, S.; Kawachi, A.; Tamao, K. *Organometallics* **2006**, *25* (26), 6142–6148.
- (2) Blicke, F. F.; Hotelling, E. B. *J. Am. Chem. Soc.* **1954**, *76* (20), 5099–5103.
- (3) I. Prisécaru, *WMOSS4 Mössbauer Spectral Analysis Software*, www.wmoss.org, 2009–2016.
- (4) Magee, T. A.; Matthews, C. N.; Wang, T. S.; Wotiz, J. H. *J. Am. Chem. Soc.* **1961**, *83* (15), 3200–3203.
- (5) Sheldrick, G. M.; IUCr. *Acta Crystallogr., Sect. A: Found. Crystallogr.* **2008**, *64* (1), 112–122.
- (6) Dolomanov, O. V.; Bourhis, L. J.; Gildea, R. J.; Howard, J. A. K.; Puschmann, H. *J. Appl. Crystallogr.* **2009**, *42* (2), 339–341.
- (7) Gaussian 09, Revision A.02, Frisch, M. J.; Trucks, G. W.; Schlegel, H. B.; Scuseria, G. E.; Robb, M. A.; Cheeseman, J. R.; Scalmani, G.; Barone, V.; Mennucci, B.; Petersson, G. A.; Nakatsuji, H.; Caricato, M.; Li, X.; Hratchian, H. P.; Izmaylov, A. F.; Bloino, J.; Zheng, G.; Sonnenberg, J. L.; Hada, M.; Ehara, M.; Toyota, K.; Fukuda, R.; Hasegawa, J.; Ishida, M.; Nakajima, T.; Honda, Y.; Kitao, O.; Nakai, H.; Vreven, T.; Montgomery, J. A., Jr; Peralta, J. E.; Ogliaro, F.; Bearpark, M. J.; Heyd, J.; Brothers, E. N.; Kudin, K. N.; Staroverov, V. N.; Kobayashi, R.; Normand, J.; Raghavachari, K.; Rendell, A. P.; Burant, J. C.; Iyengar, S. S.; Tomasi, J.; Cossi, M.; Rega, N.; Millam, N. J.; Klene, M.; Knox, J. E.; Cross, J. B.; Bakken, V.; Adamo, C.; Jaramillo, J.; Gomperts, R.; Stratmann, R. E.; Yazyev, O.; Austin, A. J.; Cammi, R.; Pomelli, C.; Ochterski, J. W.; Martin, R. L.; Morokuma, K.; Zakrzewski, V. G.; Voth, G. A.; Salvador, P.; Dannenberg, J. J.; Dapprich, S.; Daniels, A. D.; Farkas, Ö.; Foresman, J. B.; Ortiz, J. V.; Cioslowski, J.; Fox, D. J. Gaussian, Inc., Wallingford CT, 2016.